CLAS-NOTE 95-010
June 29, 1995

DEVELOPMENTAL TESTING OF A LASER CALIBRATION SYSTEM FOR THE CLAS TIME-OF-FLIGHT SCINTILLATION COUNTERS

Chris Taggart

1. BACKGROUND AND GOALS

1.1 BACKGROUND ON CEBAF AND CLAS: The Continuous Electron Beam Accelerator Facility (CEBAF) is comprised of a super conducting electron accelerator which will deliver independent beams to three experimental stations, each with its own specific purpose and detector setup. These three stations and their respective detectors are:

Hall A: two high resolution spectrometers

Hall B: large acceptance spectrometer

Hall C: high momentum magnetic spectrometer and short orbit hadron spectrometer

This research deals with the development of a detector system within Hall B: the CEBAF Large Acceptance Spectrometer (CLAS). The CLAS detector is designed to accommodate experiments involving several uncorrelated particles in the hadronic final state, or where the luminosity is limited by beam, target or accidental background. The following is a picture of Hall B..

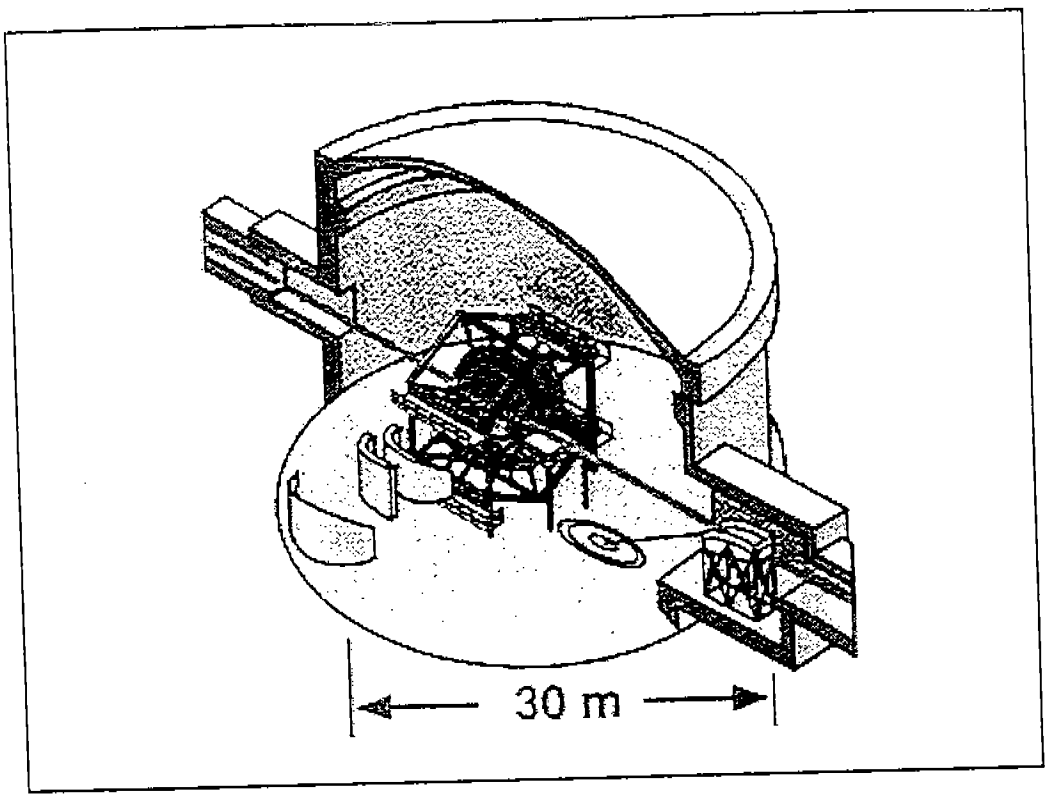

FIGURE 1. HALL B AND CLAS

In the illustration we see a cross section of the Hall B end station with the CLAS detector inside. The detector itself consists of a toroidal multi-gap spectrometer with six superconducting coils surrounded by several layers of detectors which accomplish particle detection. These detector layers include:

Drift Chambers - for measuring trajectories of charged particles

Cherenkov Counters - for electron identification

Scintillation Counters - for trigger and time-of-flight measurements

Electromagnetic Shower Calorimeter - for photon and electron detection

The following illustration shows how these detectors are arranged in the CLAS system.

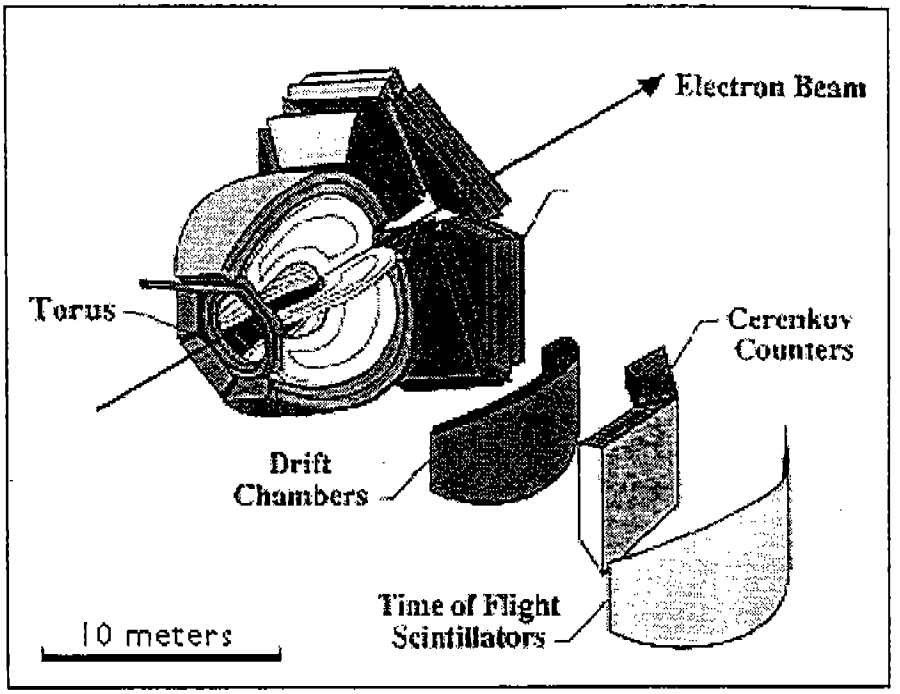

FIGURE 2. DETECTOR LAYERS OF CLAS

As illustrated, the electron beam hits the target inside the toroidal magnet. The final state particles are then tracked and identified by a layer of drift chambers, a layer of Cherenkov counters, a layer of scintillation counters, and finally a layer of electromagnetic calorimeters.

1.2 TIME-OF-FLIGHT COUNTERS: As stated above, one of the several banks of detectors in CLAS is a layer of scintillation counters. These counters play a dual role in the CLAS system. First, the first level trigger requires a scintillator hit to select particles scattered into the angle corresponding to that scintillator; and second, the counters provide time-of-flight information necessary for particle identification. The scintillators are at a fixed distance from the target, so by measuring a particle's time of flight from the target to these counters one can determine the particle's velocity. Particle identity is then deduced using this measured velocity in conjunction with the particle momentum obtained from magnetic analysis.

Each of the six sectors in CLAS contains 57 of these counters; there are thus 342 scintillators in all.

1.3 LASER-CALIBRATION: The research described in this paper involves the development of a laser-based calibration system for these 342 time of flight counters. Such a calibration system involves the simultaneous activation of these counters with pulsed laser light. This calibration scheme plays a dual role in the scintillator system. First, activation of the counters provides a relative time reference (t_0) against which all time measurements by the counters are made. In order for this activation to occur, the laser must deposit sufficient light into each of the counters to produce a signal greater than that of a minimum ionizing energy particle. Second, activation of individual counters with laser pulses of multiple amplitudes provides the necessary information to correct, in software, for the "time-walk" caused by the use of leading edge discriminators. The system must therefore be able to deposit several different amounts of laser light to each counter.

1.4 TIME WALK: Time walk is a term referring to a variance in time measurement when using leading edge discriminators. A leading edge discriminator is a device designed to generate an electrical pulse when the voltage on its input exceeds a certain threshold. This fixed threshold condition causes timing variation with respect to pulse height for pulses with a fixed rise time. This behavior is illustrated in the following diagram.

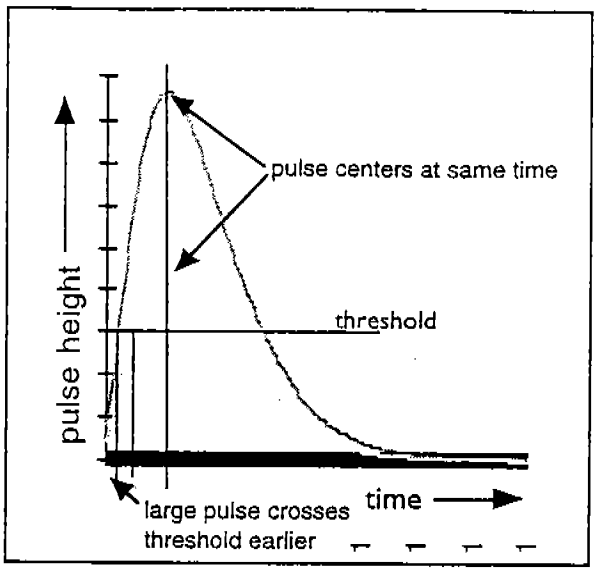

FIGURE 3. TIME WALK

Here we have two typical phototube pulses, one with amplitude of twice the other. With a leading edge discriminator set at a threshold as labeled in the diagram, we see that even though the peaks of the pulses are simultaneous, the pulse voltages cross the threshold at different times. If we were to measure arrival times of these pulses with a leading edge discriminator, we would observe that the pulse of larger amplitude arrives earlier when we should instead measure them as simultaneous. This is the discrepancy which we call "time walk." One can also see from figure 3 that if the threshold level is increased, the time discrepancy beween the two pulses becomes more significant. Thus, for higher discriminator threshold levels a time walk correction of greater magnitude is required.

There are devices, referred to as constant fraction discriminators, which automatically account for this effect with a clever electronic circuit. Constant fraction discriminators do not use a fixed leading edge threshold, but are rather fired when the input voltage reaches some constant fraction of the total pulse height. This trigger condition makes the time of generating a discriminator pulse independent of pulse height. However, constant fraction discriminators are expensive. When the pulse

height is also measured, empirical software corrections to leading edge discriminator times acheive comparible time resolution.

1.5 PREVIOUS RESEARCH: This project builds upon previous research (performed by T.G. Pavey and R. Perez at the College of William and Mary in 1993) dealing with the very same laser calibration system. Their work focused primarily on the first requirement of the calibration system: sufficient light deposition in the counters. The system built and tested by Pavey and Perez consisted of a pulsed nitrogen laser whose beam was divided by a series of two fiber optic splitters. The split beam was then shined into a piece of scintillator and by using a radioactive source as a calibration, the amount of light deposition into the counter was measured.

The results of Pavey and Perez's work unfortunately fell short of the necessary light deposition requirement. The minimum ionizing energy deposited in the scintillators in the CLAS time of flight system is about 10MeV, but the system which they built would only deposit enough light to produce a signal equivalent to about 2 MeV. A sufficient amount of light was simply not reaching the counter after the splitting.

Several possible factors could account for the inadequacy of their system. The laser used in their research (Laser Photonics LN120) was a very unreliable spark gap driven unit which required constant maintenance and repair and was most likely not working at an optimum performance level. The efficiency of the optical system used to transfer the laser light into the fiber optic splitters could also account for a significant source of light loss. The roughness of connections between fibers in the system was also proposed by Pavey and Perez as a source of light loss, but the consistency of their energy measurements from all fibers in the splitters suggests that this loss was not that significant. If there were significant losses due to bad fiber connections, one would expect to see great variation in the amount of light coming from each fiber in the splitter system. Their measurements suggested otherwise.

1.6 GOALS OF THIS RESEARCH: This research is intended to accomplish two real goals. Firstly, improvements are to be made upon the system built by Pavey and Perez to increase the amount of laser light deposited to each of the counters. These improvements include the use of a more reliable and more powerful thyrotron-driven pulsed nitrogen laser (Laser Photonics LN 203C)as well as the use of a commercially produced connector designed to transfer the light from this laser into an optical fiber. It is hoped that these improvements will reduce light loss as described above due to laser performance and optical inefficiency as described above. A new measurement of light deposition is to be made with these improvements.

Second, this research involves an empirical assessment of the system's ability to correct for time walk. The pulsed laser and optical fiber system are used in conjunction with actual scintillation counters from the CLAS time of flight system to try to correct for time walk in a set of experimental data.

2. DESCRIPTION OF EXPERIMENT

2.1 EXPERIMENTAL OUTLINE: With two goals described in the previous section in mind, the following experimental scheme was developed.

Accomplishment of the first goal, assessment of time walk correction in a counter, requires the following information:

1. the functional relationship between pulse height and time of pulse arrival for that counter (We will call this the time-walk correction function.)

2. a set of actual experimental data from the counter, taken with leading edge discriminators, to which the deduced time walk correction function can be applied

3. a set of experimental data for the same experimental conditions taken with constant fraction discriminators (This acts as a control set to which the corrected leading edge data are compared as an assessment of the correction's effectiveness. The goal is to correct the time distribution of the data taken with leading edge discriminators so that it resembles that taken with the constant fraction discriminators.)

Accomplishment of the second goal of measuring the amount of light arriving at the scintillator from the fiber system requires the following data.

1. spectra showing the pulse height corresponding to arrival at the detector of known fractions (through filtration) of the laser's full beam

2. an energy calibration spectrum against which the laser pulse data can be compared (This direct comparison will determine if the amount of light reaching the scintillator is enough to excite it adequately for calibration.)

Based upon the above required pieces of information, the following experimental scheme was devised. Light pulses from a nitrogen laser would be fed via an optical fiber into one of the scintillators from the time of flight system. The system would be designed such that various filters could be placed in the beam before it enters the fiber, allowing known fractions of the total beam to reach the counter. With this configuration, pulse height and timing data could be obtained from the counter for various amounts of deposited light. This would provide the data needed to determine the time walk correction function and the pulse height for known amounts of laser light as mentioned above. The other required data sets would be provided by obtaining cosmic ray spectra with the same counter. Cosmic ray data can be used both as a means of measuring the counter's minimum ionizing energy for assessment of light deposition, and as actual experimental data to which the time walk correction function can be applied.

Thus, we have the following experimental outline:

1. Obtain pulse height and timing data for the counter as it is activated by laser pulses of varying intensities.

2. Obtain cosmic ray spectra from the same counter using both constant fraction and leading edge discriminators to trigger timing measurements.

3. Deduce the time walk correction function from the data in step 1.

4. Apply the function to the leading edge data in step 2 and assess the correction's effectiveness by comparison with the corresponding constant fraction data.

5. Use the cosmic ray data as an energy calibration to determine the amount of light reaching the scintillator in step 1.

6. Evaluate the proposed system based upon the amount of light deduced in step 5.

2.2 EXPERIMENTAL SETUP: The following is a general schematic diagram of the experimental setup used to obtain the data described above.

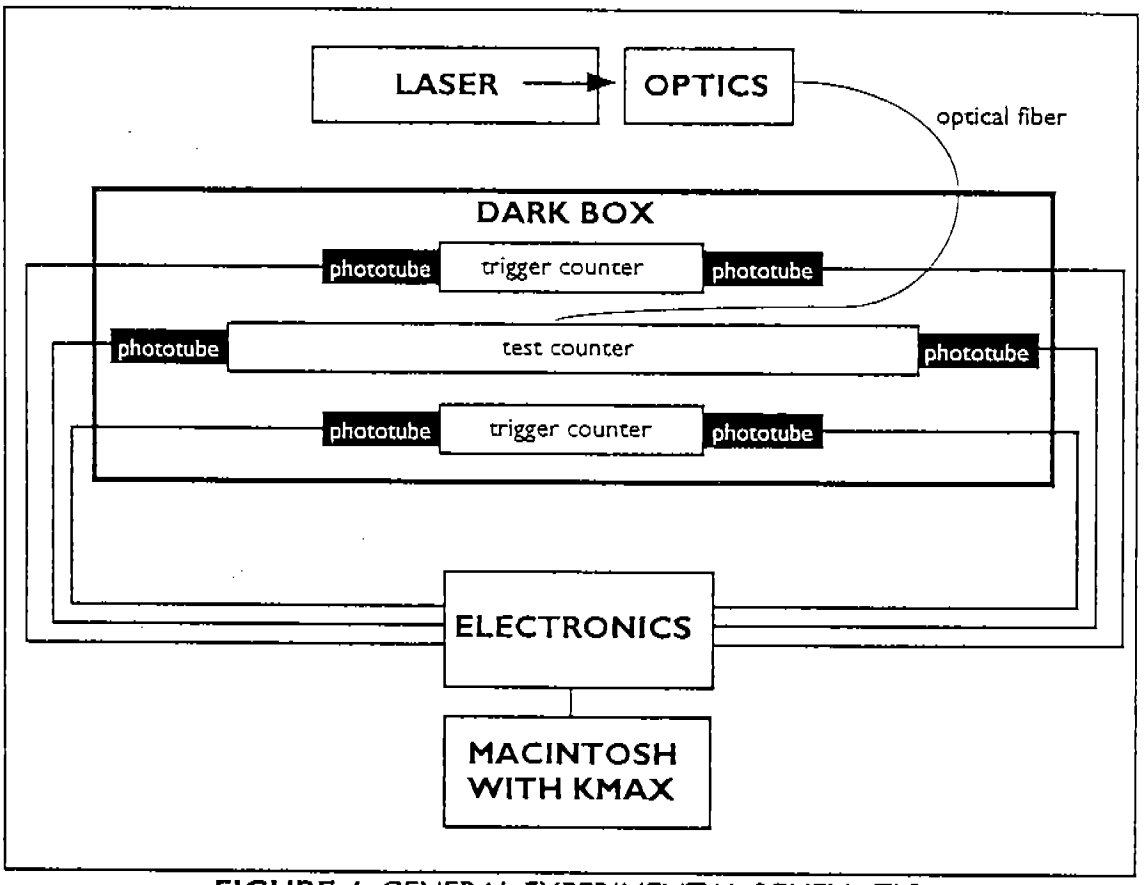

FIGURE 4. GENERAL EXPERIMENTAL SCHEMATIC

As one can see, the system involves three scintillation counters, all of which are detectors to be installed as part of the CLAS time of flight system. These are mounted inside a dark box for the duration of the experiment. Two small counters, which we will call the trigger counters, are positioned above and below a larger counter, which we will call the test counter. All three counters are made of 5 cm-thick Bicron BC-408 scintillator. The trigger scintillators are 15 cm wide by about 30 cm in length, and the test scintillator is 20 cm wide by 200 cm in length. As pictured, each is coupled to a pair

of photomultiplier tubes, one situated at each end. Coupled to the trigger counters are EMI 9954A phototubes. Coupled to the test scintillator are Phillips XP4312B 3-inch phototubes. High voltage is applied to each tube individually and anode signals from each are fed into electronics (to be described in detail later). Data are then recorded from the electronics using an automated KMAX data acquisition system on a Macintosh computer. KMAX is a commercially produced software package used for recording and analyzing data from experimental instrumentation.

This same experimental setup is used to collect both the cosmic ray data sets and the laser data sets as described above. The trigger counters are used only as a trigger in the cosmic ray data sets and are not used in the laser sets.

2.3 DETAILS OF EXPERIMENTAL SETUP: The following is a detailed schematic of the laser and optics in the system.

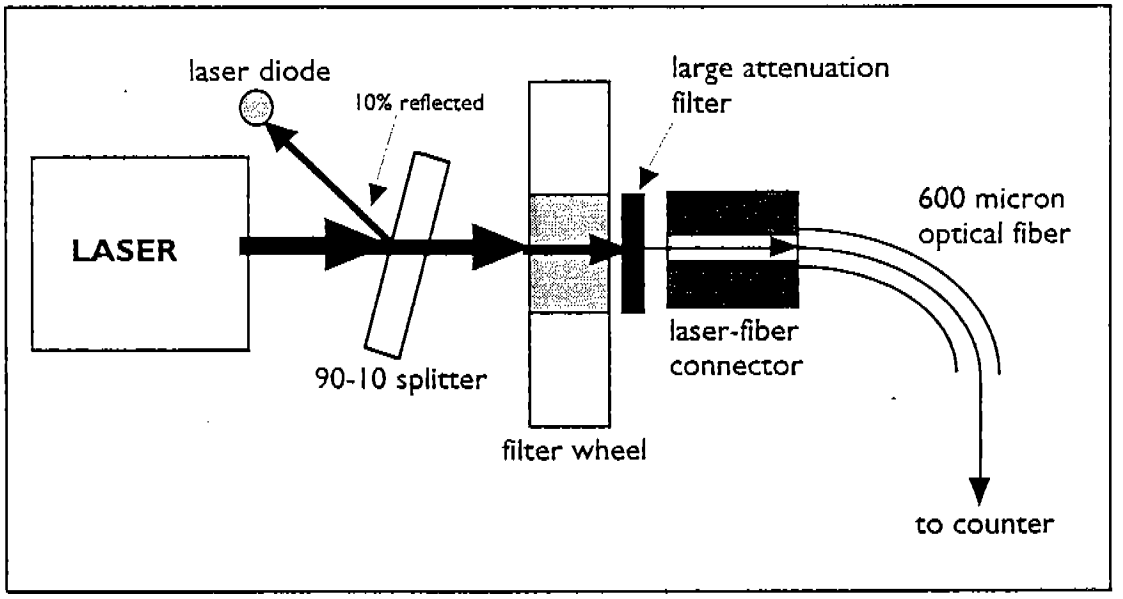

FIGURE 5. DETAILED OPTICAL SCHEMATIC

As pictured, the light from the pulsed nitrogen laser progresses through several optical devices before entering the optical fiber. It passes first through a 90-10 splitter

filter which reflects back 10% of the beam and allows 90% to pass. The reflected 10% reaches a laser diode which provides a fast negative signal when exposed to laser light. This diode acts as the trigger for data taken using the laser. The beam then passes through a changeable filter wheel. This wheel contains five different filters which can be easily changed to vary the amount of laser light entering the fiber. The filters are numbered 1 through five with #5 allowing the most light to pass and #1 allowing the least. The exact attenuation of these filters is not known, but it is assumed that they allow amounts of light to pass proportional to their number (i.e. filter #5 would pass 90%, #4 would pass 70%, #3 would pass 50%, etc.). Because the laser is being fired into only one scintillator in this experiment without being divided, an additional filter is added after the filter wheel to greatly reduce the amount of beam. This filter, which was simply attatched to the filter wheel in the beam line with a piece of adhesive tape, had an attenuation of 10^4 (one ten-thousandth of the beam's light passes through). After passing through the various filters the beam enters a special laser-to-fiber connector manufactured by the company that built the laser. It is designed to direct the light from this laser into a 600 micron optical fiber. This fiber is then fed to the test scintillator such that it shines into the midway point between the counter's two phototubes.

The following drawings show the design for the mountings which were built to hold the various optical devices described above.

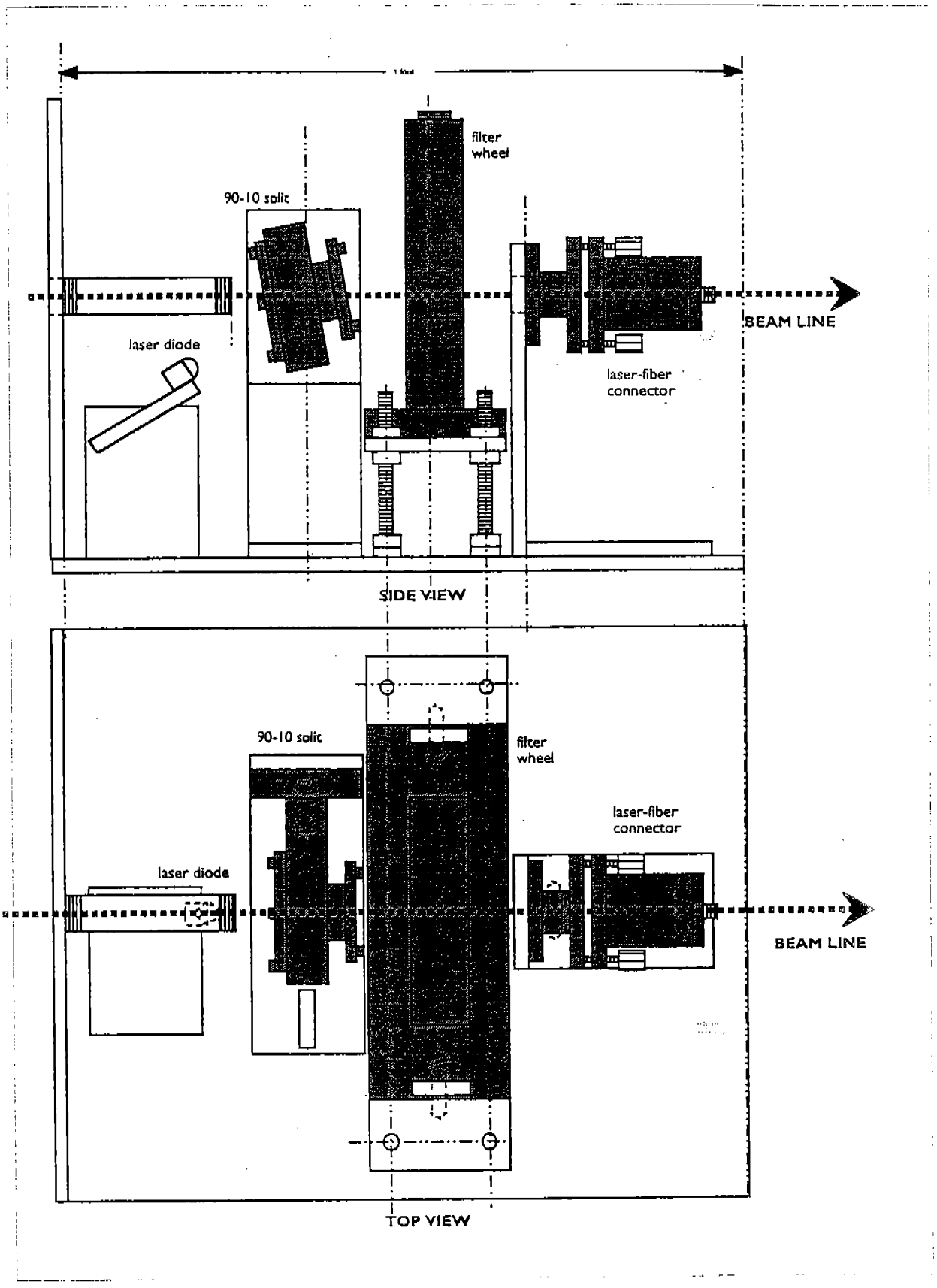
filter
wheel
90-10 split
laser diode
laser-fiber
connector
BEAM LINE
SIDE VIEW
90-10 split
filter
wheel
laser-fiber
connector
laser diode
BEAM LINE
TOP VIEW

These mountings were constructed from aluminum stock at William and Mary. The short piece of threaded pipe shown at the left side of the drawing is used to reduce noise coming from the box in which the laser sits. The entire optical mounting setup is surrounded by an aluminum cover making the beam totally enclosed. The beam enters the box at the left from the laser, which is itself closed in an aluminum box, and leaves the right side of the optics enclosure by means of the optical fiber.

The six phototubes which see the scintillation counters are named, for reference, as shown in the following diagram.

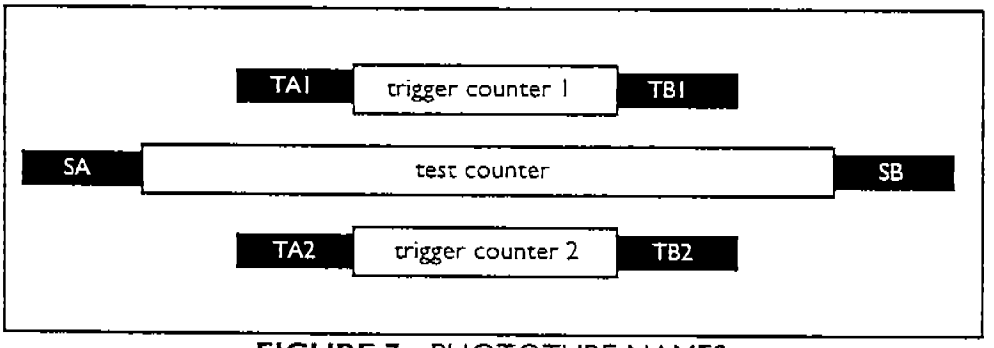

FIGURE 7. PHOTOTUBE NAMES

The top trigger scintillator is named trigger counter number 1 and the bottom is named number 2. The left and right tubes for trigger counters 1 and 2 are named TA1, TB1, TA2, and TB2, respectively. The left and right tubes on the test counter are named SA and SB, respectively. The following diagram illustrates in detail the electronics used to interpret the anode signals from the phototubes.

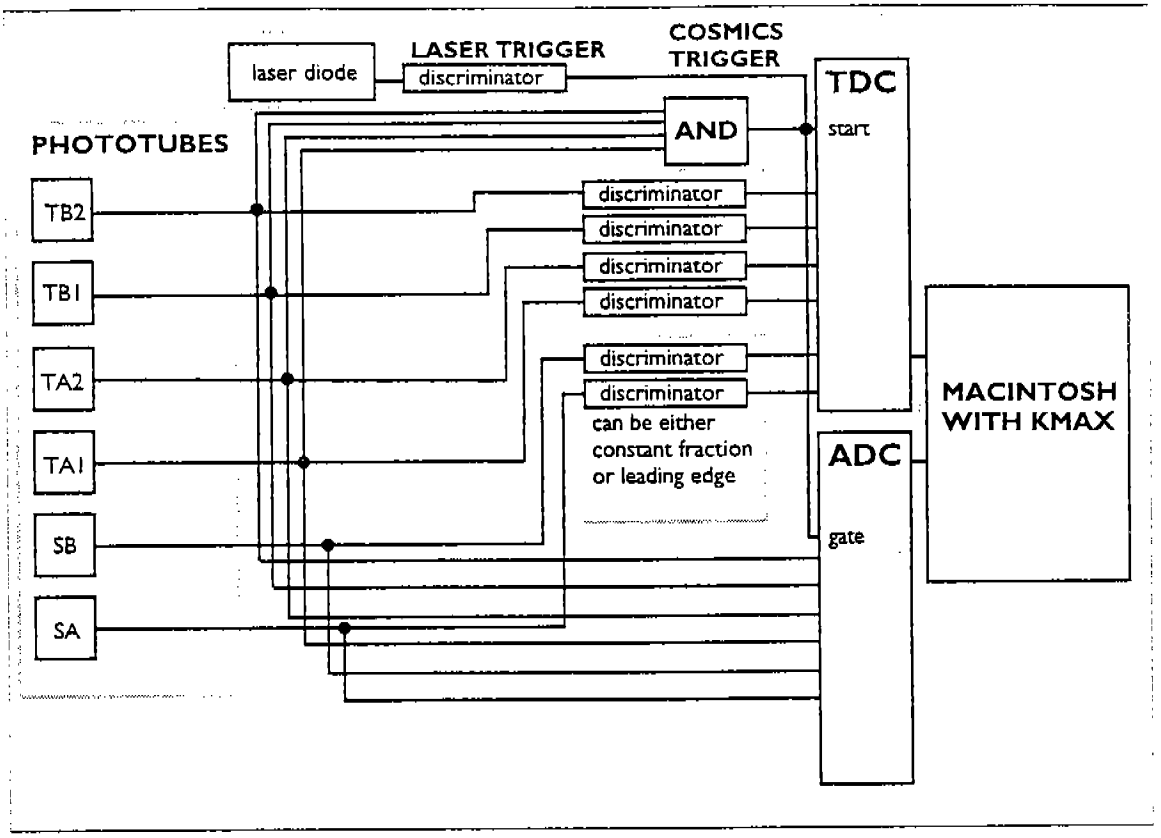

FIGURE 8. ELECTRONICS SCHEMATIC

As pictured, each phototube anode signal is split and fed into an Analog to Digital Converter (LeCroy 2249W ADC) and into a discriminator whose output feeds a Time to Digital Converter (Le Croy 2228A TDC). The discriminators firing the TDC inputs corresponding to the tubes of the test scintillator can be changed between constant fraction and leading edge (Phillips 711 for leading edge and SIN T87 for constant fraction). For cosmic ray data sets, the start for the TDC and gate for the ADC are provided by establishing an AND (Phillips 756 4/4) signal from the four tubes on the trigger counters. For laser data sets the TDC start and ADC gate are provided by a discriminator signal fed by the laser diode. Thus, for each triggered event during a data run, the pulse height and time of pulse arrival with reference to a trigger from either the trigger counters (for cosmic rays) or the laser diode (for laser data) are recorded for all six phototubes. For laser data runs the signals from the trigger counters are recorded, but ignored in analysis.

2.4 EXPERIMENTAL PROCEDURES: The following section outlines the procedures performed to obtain the data sets with the system described.

Before taking experimental data several preliminary adjustments were made. Nitrogen gas flow to the laser cavity was increased to a maximum to allow for a high pulse repetition rate (50 Hz). The voltages on phototubes SA and SB were then adjusted so that both had approximately the same gain (i.e. pulse heights from both tubes would be of about the same amplitude for any given particle passing through the counter). The final voltages for these tubes were 1950 volts for SA and 2100 volts for SB.

The first series of data sets was then taken. The SA and SB signals were fed into leading edge discriminators whose thresholds were set at 100mV. The start of the TDC and ADC gate were provided by the discriminator pulse triggered by the laser diode. The filter wheel was then set at level one and the laser was turned on. Data were then collected for about 1000 events and saved to disk. The filter wheel was then stepped through all five settings, and a separate data set of 1000 events was recorded for each setting.

The laser was then turned off and the trigger was changed from the laser diode to the OR output of tubes TA1, TB1, TA2, and TB2 (the tubes on the test counter). The discriminators were left as leading edge with the same threshold level of 100 mV. The system was now ready for detecting cosmic rays. A cosmic ray spectrum was then taken for 1000 events and saved to disk.

The discriminators were then changed from leading edge to constant fraction and the thresholds were set at 100 mV. Another cosmic ray data set was then obtained and saved to disk.

At this point 1000-event data sets were taken for each of the 5 filters with leading edge discriminators, for cosmic rays with leading edge discriminators, and for

cosmic rays with constant fraction discriminators. The same process was then repeated with the discriminator levels changed to 50 mV instead of 100 mV to see if the low-pulse height events in the data sets were being affected by the threshold. After this process was repeated there were 14 data sets in all saved to disk.

3. DATA ANALYSIS

3.1 THE RAW DATA FILES: The data files saved in the above data runs contain 17 pieces of information for each event recorded. For example, a sample line of data for a particular event in a file might look like this (This is one of the 1000 lines of data from a cosmic ray data set taken with constant fraction discriminators at a threshold of 50 mV.):

562 349 267 348 344 811 586 255 98 345 605 414 477 372 38 484 259

The first number is the event number, so all data in this line corresponds to event #562 out of the 1000 events in the data set. The next six numbers are the TDC values for tubes TA1, TB1, TA2, TB2, SA and SB, respectively. The six numbers following those are the corresponding ADC values for each of the tubes TA1, TB1, TA2, TB2, SA and SB, respectively. The 14th and 15th values in the series are calculated values based upon the TDC values which are not important to this particular experiment. (Other tests were being performed with the same experimental setup which utilized these values.) The last two numbers are calculated values which are important in understanding cosmic ray timing in this system. They are the TDC values from SA and SB, respectively, minus a reference time T_{REF} which adjusts time values so

that timing from different events all lies on the same time scale. T_{REF} is calculated as follows.

First, the time at which a particle passes through each of the trigger scintillators is calculated. We call these times T_1 and T_2 for trigger counters 1 and 2, respectively. The time at which a particle passes through a trigger scintillator is the average of the times of the two phototubes of that counter. Thus:

$$T_1 = \frac{TA1+TB1}{2}$$
$$T_2 = \frac{TA2+TB2}{2} \qquad (1)$$

We then define the reference time T_{REF} as the time at which the particle passes through the test scintillator. This is just the average of the mean times T_1 and T_2. Thus:

$$T_{REF} = \frac{T_1+T_2}{2} = \frac{TA1+TB1+TA2+TB2}{4} \qquad (2)$$

This time iprovides an accurate reference time independent of the position at which the particle passes through the trigger scintillators. The last two values in the sample data line are simply the TDC values for tubes SA and SB minus this reference time. As an example, we calculate the last value SB-T_{REF} in the data line.

$$SB - T_{REF} = SB - \frac{TA1+TB1+TA2+TB2}{4} = 586 - \left(\frac{349+267+348+344}{4}\right) = 259 \qquad (3)$$

As one can see this is in fact the last value in the sample data. These corrected timing values are only important in dealing with the cosmic ray data sets. For the laser data sets, the trigger from the laser diode is always at a known time, so no such adjustment is needed. The only data values which are relevant in the laser data sets are

the ADC and TDC values for tubes SA and SB. All others are only applicable to the cosmic ray data.

3.2 DETERMINATION OF PEDESTAL VALUES: The first preliminary step in the data analysis was to determine the position of the pedestal values for the ADC spectra taken for tubes SA and SB. This pedestal must be subtracted from each data point as a zero reference. To determine the pedestal values, laser data sets were taken with the beam still reaching the laser diode trigger, but with the fiber disconnected from the laser to fiber connector such that no laser light actually hit the counter. The small amplitude events from tube noise would accumulate in the pedestal bin of the ADC spectra. From this procedure it was determined that the ADC pedestal bin numbers for SA and SB were 65 and 55, respectively. These values were subtracted from all ADC values in analyzed data sets.

2.2 DETERMINATION OF DISCRIMINATOR THRESHOLD POSITIONS: The next preliminary step involved the determination of the ADC bin corresponding to the discriminator threshold values of 50 and 100 mv. This procedure involved taking a spectrum for small amplitude laser pulses and increasing the threshold to several high values. A software filter was applied using KMAX to the ADC spectrum such that no event would be shown if the TDC was not fired (i.e. the pulse was lower than the discriminator threshold.). This spectrum would be cut off on the low end in comparison to the ADC spectrum without the filter applied. The following cutoff bin positions were measured for the following three discriminator threshold values:

TABLE 1: THRESHOLD VALUES AND CUTOFF BIN NUMBERS

threshold (mV)	cutoff bin
100	114
125	119
150	124

Assuming the ADC behaves with a linear relationship between voltage and bin number, we can deduce from the above data the following relation between bin number and threshold value:

$$\text{Bin\#} = 94 + 0.2(\text{threshold}) \tag{4}$$

From this low-statistics estimate of the relationship we can estimate the bin number of the two threshold levels used in this experiment: 50 and 100 mv. For 100 mV we obtain bin number 114 and for 50 mV we obtain bin number 104. The pedestal values must be subtracted from these bin numbers like any other ADC value, so we obtain the following threshold bin numbers for the two tubes.

TABLE 2: CUTOFF BIN NUMBERS FOR TUBES

TUBE	50 mv bin#	100 mV bin#
SA	39	49
SB	49	59

For events with pulse height near these thresholds there will be inconsistencies due to some events being cut off by the threshold. Events which have ADC values near these thresholds will be ignored in analysis to improve accuracy.

3.4 DETERMINING THE TIME WALK CORRECTION FUNCTION:

The next step in the analysis is to determine the relationship between pulse height and time of pulse arrival in the laser data sets. This relationship will lead to the time walk correction function to be applied to the cosmic ray spectra. In order to determine this function we must plot the relationship between TDC and ADC values for the events in the laser data sets with different filters. The following is one such plot:

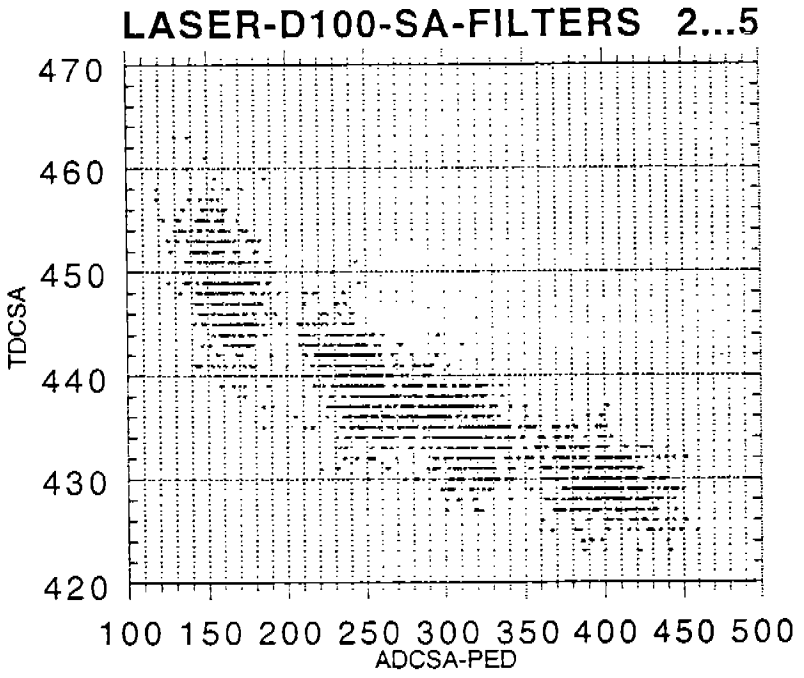

This plot shows the TDC values for laser events compared with their corresponding ADC values minus the pedestal. Compiled in this plot are events from data sets taken with tube SA for filters two through five with the discriminator thresholds set at 100 mV. Data from filter number one were ignored because most of the events had small pulse-heights near the discriminator threshold level.

Such plots were made for each tube for both threshold levels. Data from filter number one were ignored in all cases because these sets all contained a significant number of events near the threshold level.

To determine the time walk correction function we must fit a curve to these data which we can then apply to experimental data. Two functional forms are to be used as fits to the data. They are

$$TDC = m_1 + \frac{m_2}{\sqrt{ADC}} \tag{5}$$

and

$$TDC = m_1 + m_2 \ln(ADC) + m_3 \ln(ADC)^2 \tag{6}$$

Here m_1, m_2 and m_3 are parameters used in curve fitting. The first of these two forms (5), which we will refer to as Fit #1, can be derived from the shape of an average photomultiplier pulse. By integrating the total charge delivered by the pulse to a TDC through time one can deduce the inverse square root relationship between time and pulse height[1]. The second form (6), which we will call Fit #2, is a more general version of the first which is said to be more accurate in making time walk corrections for actual experimental data with wide pulse height ranges[2].

The following plots show the data plotted above with fit results using both fits #1 and #2. All fits were performed using Kaleidagraph, a commercially produced graphing and analysis program for the Macintosh computer.

---

[1]Refer to "Application Note AN-5: Time-of-flight Measurements and Leading Edge Timing Compensation", LeCroy Corporation, New York, 1983.

[2]Refer to S. Banjeree et al., "Design and Performance of a Time-of-Flight System for Particle Identification at the Fermilab Collider", **Nuclear Instruments and Methods in Physics Research**, A269, 1988, p129.

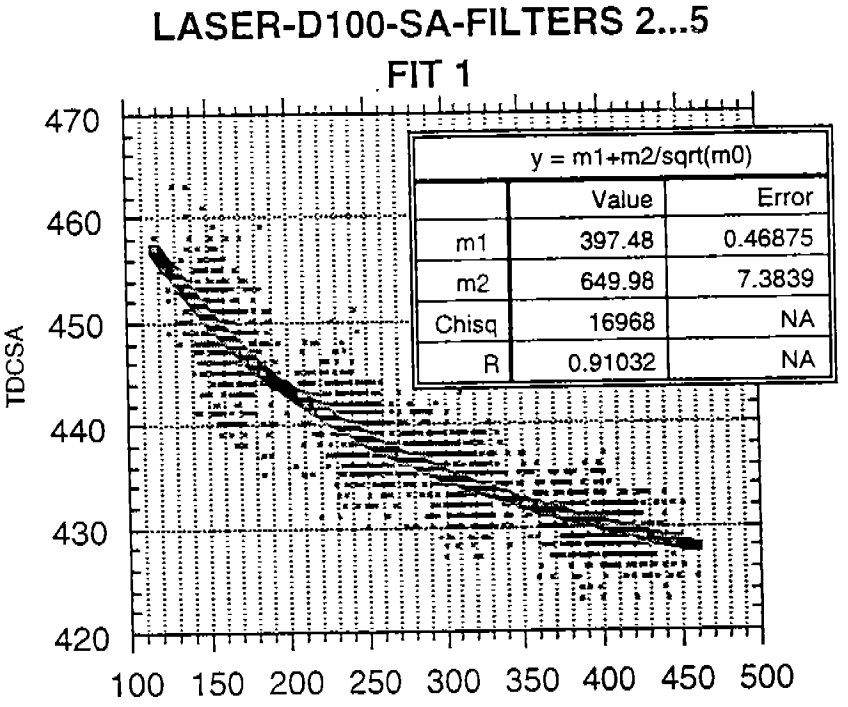

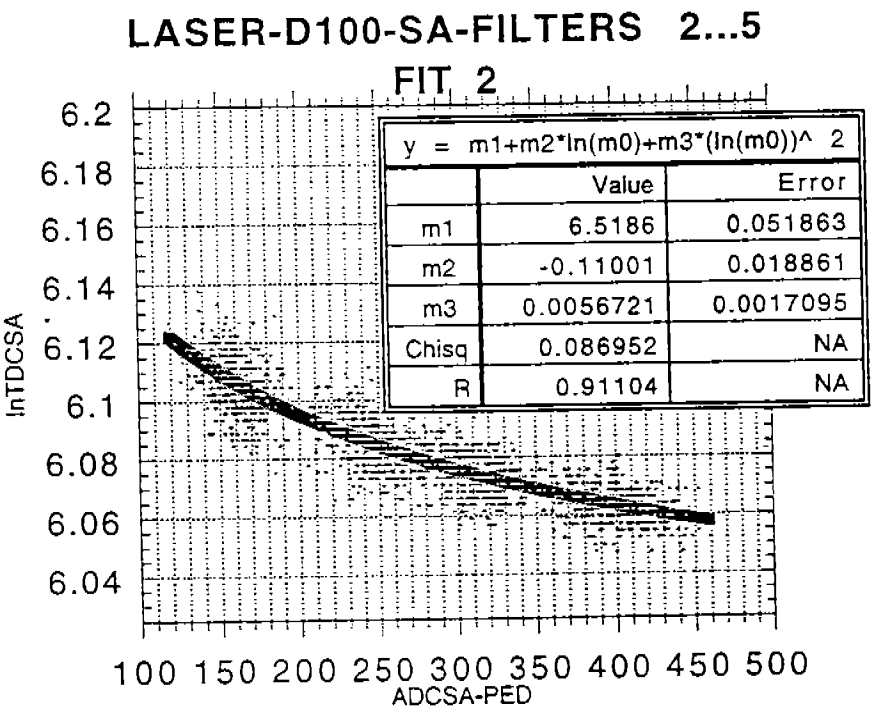

In the second plot the TDC scale has been changed to a natural log of the TDC value in order to make fitting the second functional form easier. From the two fits

shown above we have obtained the relationships between pulse height and timing for tube SA with a discriminator level of 100 mV. They are:

$$TDC = 397.48 + \frac{649.98}{\sqrt{ADC}} \tag{7}$$

for fit #1 and:

$$\ln(TDC) = 6.51860 - 0.11001(\ln(ADC)) + 0.0056721(\ln(ADC))^2 \tag{8}$$

for fit #2.

Such fits were performed using both functional forms on all laser data sets obtained in the procedure. All such plots with their fits are compiled in **APPENDIX A** at the end of this paper.

3.5 APPLICATION OF THE CORRECTION FUNCTIONS:

Now that the time walk correction functions have been determined we can apply them to the cosmic ray data sets taken. Plotted here are data from one such set:

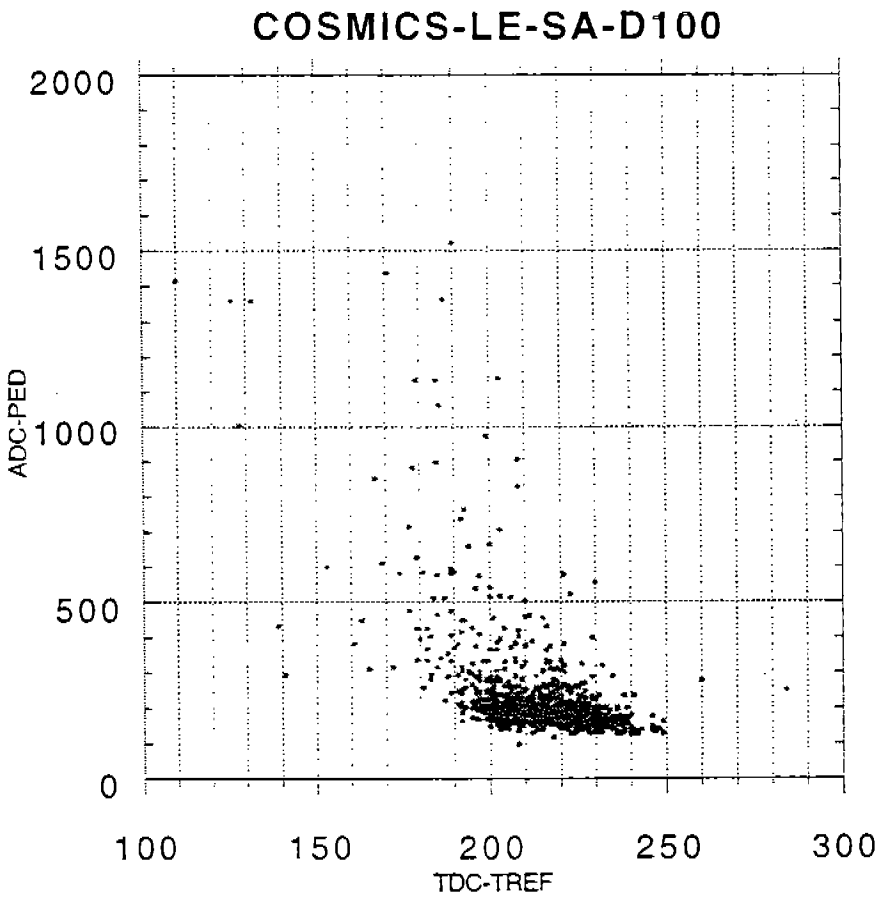

Plotted above are approximately 1000 cosmic ray events as seen with tube SA with leading edge discriminators triggering the TDC and thresholds set at 100mV. Compared are each event's ADC value with its corresponding time value (TDC minus T_{REF} as discussed previously). One can easily see that the overall distribution is skewed upwards to the left. This is behavior consistent with leading edge discriminator time walk; events with large pulse height appear to arrive earlier. The next plot shows, for comparison, similar data taken with constant fraction discriminators rather than leading edge.

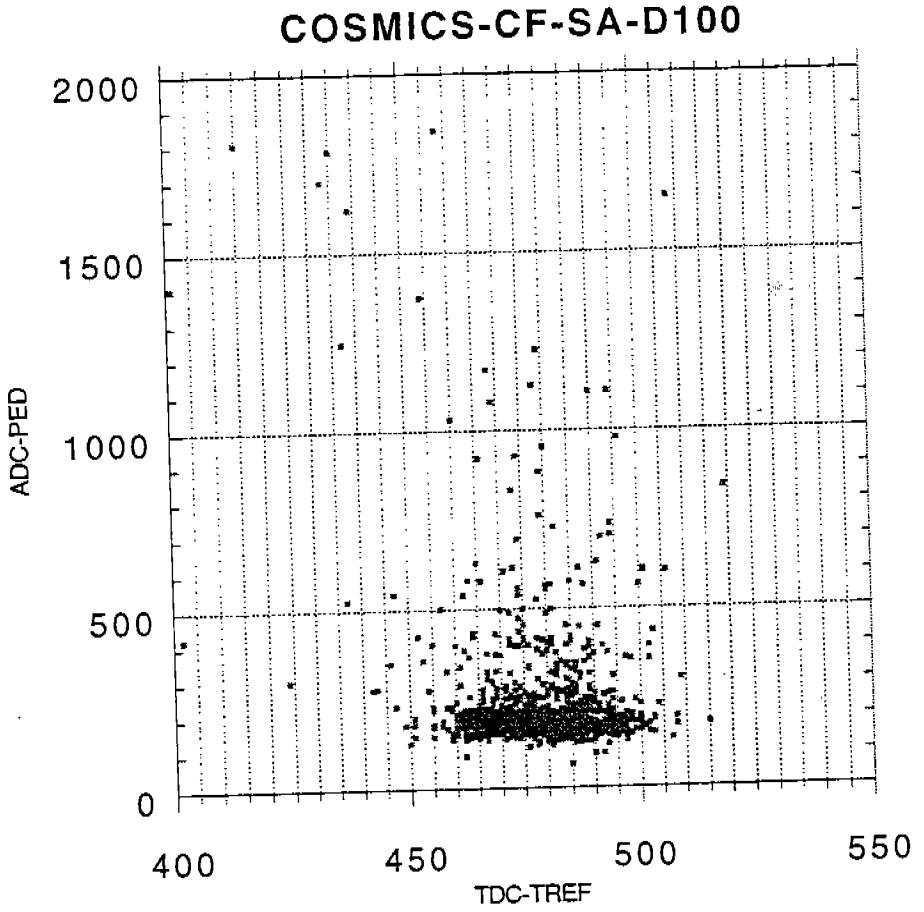

This plot shows the same comparison of cosmic ray events' ADC values to their corresponding time values from tube SA with thresholds set at 100mV. The only difference is that the discriminators have been changed to constant fraction rather than leading edge. In comparing this plot with the one previous, we see that the constant fraction discriminators are indeed doing their job of removing the time dependence of events with respect to their pulse height. The distribution in this plot shows no such dependence; it is evenly distributed in time with respect to pulse height. In comparing the time values of this plot with the leading edge plot one might notice that all events appear to come later from the constant fraction discriminator than from its leading edge

counterpart. This is due to a time delay in the actual operation of the two units. Constant fraction discriminators have a longer processing time than leading edge discriminators.

In applying the time walk correction function, the goal is to make the time distribution in the first plot like that in the second plot. One wants to remove the skewed timing, thus making the data taken from leading edge discriminators appear as if it were taken with constant fraction discriminators. The time walk correction function is applied as follows.

In the cosmic ray data sets each event has some time value which is dependent upon the event's pulse height. This time will be referred to as T_{RAW}. In order to correct T_{RAW} for time walk, we must subtract from it some correction ΔT such that a more accurate event time $T_{CORRECT}$ is determined. Thus

$$T_{CORRECT} = T_{RAW} - \Delta T \tag{9}$$

The correction ΔT is defined as

$$\Delta T = T(ADC) - T(ADC_0) \tag{10}$$

where T is the experimentally determined time walk correction function, ADC is the ADC value of the event and ADC_0 is an arbitrary reference ADC value. We then get

$$T_{CORRECT} = T_{RAW} - T(ADC) + T(ADC_0) \tag{11}$$

as the corrected time value. It is seen that the term $T(ADC_0)$ acts as an arbitrary offset to be chosen at will. The leading edge cosmic ray data plotted above can now be corrected. We refer back to equations (7) and (8), the two experimentally

determined correction functions for tube SA. These act as the function T in the correction relation above. The following plot shows events from the leading edge data set after the application of the first correction function (7).

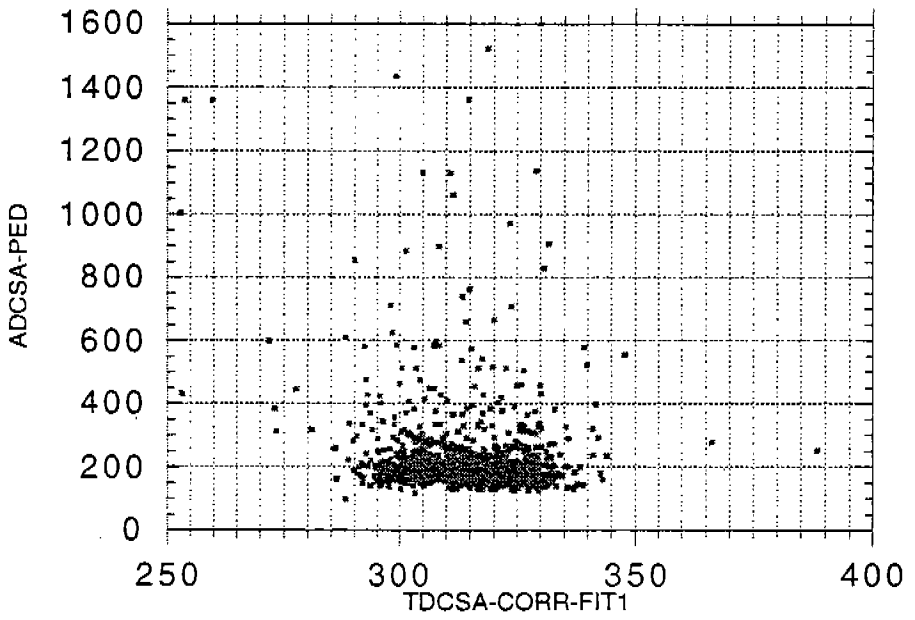

LEADING EDGE DATA CORRECTED WITH $T = 397.48 + \frac{649.98}{\sqrt{ADC}}$

In comparing this plot with the plot of similar data from the constant fraction discriminator we see that the correction function has very nicely removed the effects of time walk from the distribution. There is no tendency for larger pulses to arrive any earlier than smaller ones.

The following shows the same set of data corrected with the second experimentally determined time walk correction function (8).

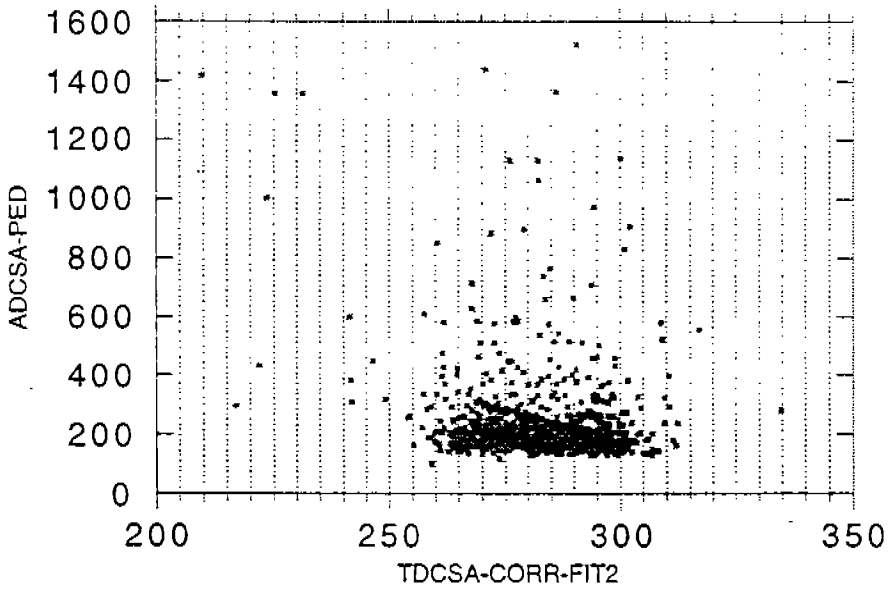

LEADING EDGE DATA CORRECTED WITH

$$\ln(T) = 6.51860 - 0.11001(\ln(ADC)) + 0.0056721(\ln(ADC))^2$$

Once again the time walk correction function has very nicely removed the time dependence with respect to pulse height in the leading edge data.

The same correction process was performed on all cosmic ray data taken with leading edge discriminators using both correction forms (5) and (6). The results of these corrections are compiled in **APPENDIX B**, along with comparisons to corresponding constant fraction data.

3.6 ASSESSMENT OF TIME WALK CORRECTION EFFECTIVENESS:

We can qualitatively asses the effectiveness of these corrections by looking at the time distributions of the corrected data and comparing them to the time distributions of data taken with constant fraction discriminators. In order to compare these time distributions effectively, however, we must first perform one more manipulation of the data.

The effects of time walk have been corrected independently in the times measured for the two phototubes on the scintillator, but there is another significant

contributor to time variation of detected events, namely the size of the area of detected cosmic rays. Any cosmic ray which passes through both trigger counters will be detected by the test counter. Thus the region of the test counter through which detected cosmic rays pass is about 30 centimeters long. The path length of emitted light from a cosmic ray event in this region to one of the phototubes at the end of the scintillators can therefore vary by up to 30 centimeters between events. This variation in length translates into a significant time variation between events (~ 2 ns). We eliminate this effect by averaging the times from the tubes at each end of the counter. Suppose a cosmic ray passes through the test 10 centimeters from the center of the counter. The distance from the event to one of the phototubes is 10 centimeters shorter than average, yet it is at the same time 10 centimeters longer than average for the other phototube. This linear relationship allows us to cancel out the time variation by simply averaging the times measured by both phototubes for the event. This mean time, which effectively places all events at the center of the counter, is independent of the event's position in the test counter. We assess the time walk correction's effectiveness in improving the time resolution of the counter by analyzing the distribution of these measured mean times.

For reference, let us first look at the distribution of event mean times for cosmic ray data taken with constant fraction discriminators. Note that in all of the following plots each TDC bin corresponds to 50 picoseconds (i.e. 1 nanosecond = 20 bins).

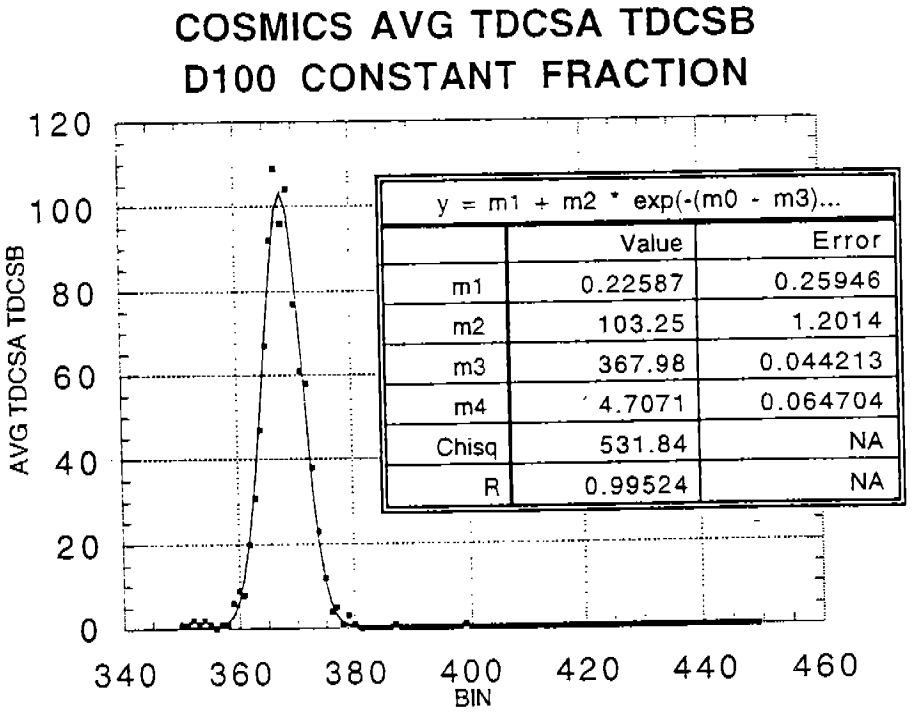

This graph shows the distribution of the mean TDC values of phototubes SA and SB for cosmic ray events using constant fraction discriminators. A Gaussian had been ft to the distribution with a parameterization as follows:

$$y = m_1 + m_2 \exp\left(\frac{-(x-m_3)^2}{m_4^2}\right) \tag{12}$$

where m_4 is related to the width σ of the distribution by

$$\sigma = \frac{m_4}{\sqrt{2}} \tag{13}$$

Thus we determine that the width σ_{CF} of the timing distribution plotted above is

$$\sigma_{CF} = \frac{4.7071}{\sqrt{2}} = 3.328 \tag{14}$$

We call this σ_{CF} the time resolution of the counter with constant fraction discriminators. With the ADC scale of 50 picoseconds per bin, this translates to σ_{CF} =166 picoseconds.

We now perform the same measurement of time resolution on the cosmic ray data taken with leading edge discriminators. The following histogram shows the

distribution of mean TDC values of phototubes SA and SB for cosmic ray events using leading edge discriminators with a threshold of 50 mV.

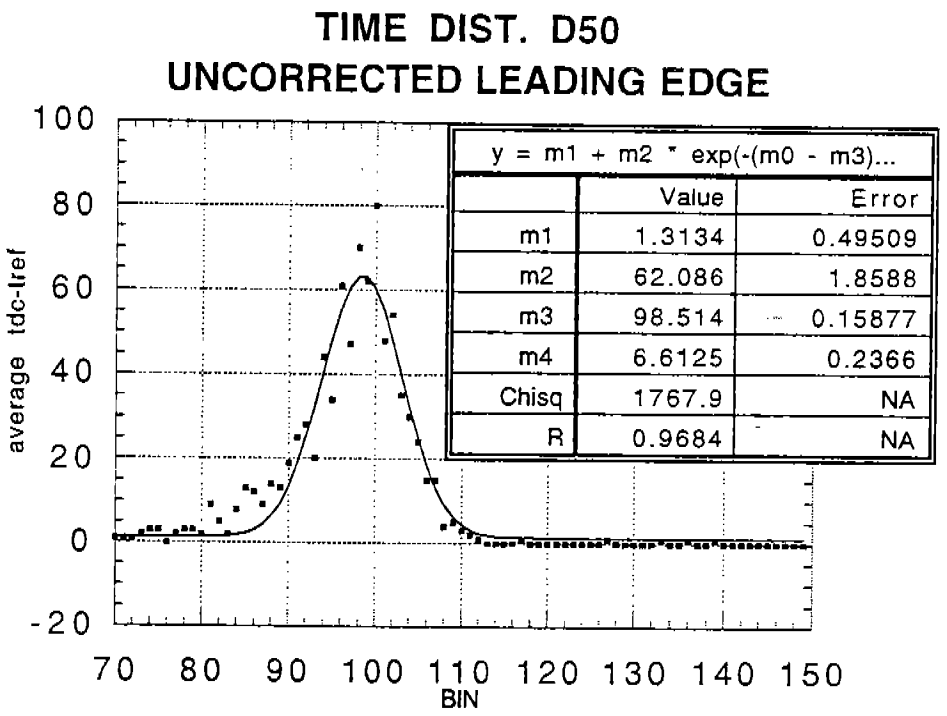

We have again fit a Gaussian to this distribution from which we deduce the resolution σ_{LE50}.

$$\sigma_{LE50} = \frac{6.6125}{\sqrt{2}} = 4.676 \qquad (15)$$

We see that the counter's resolution (σ_{LE50} = 4.676 = 234 ps) with leading edge discriminators is, as expected, much larger than with constant fraction discriminators. Next, we perform the same resolution measurement for data taken with leading edge discriminators with a threshold of 100 mV.

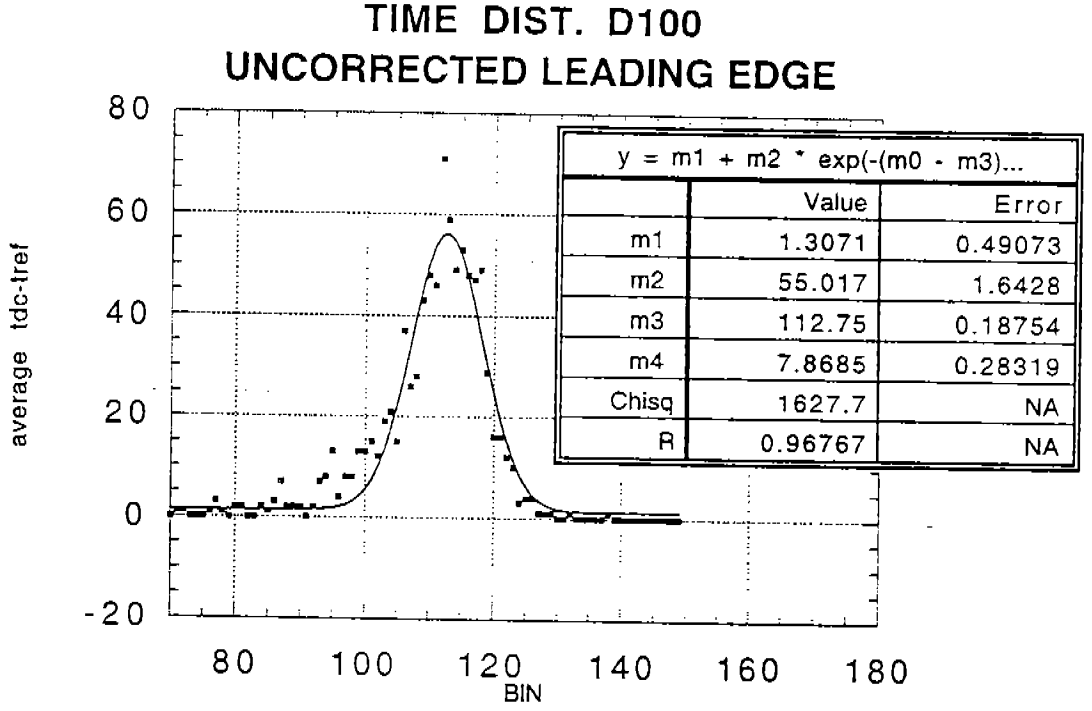

The resolution σ_{LE100} of this distribution is again determined from the Gaussian fit:

$$\sigma_{LE100} = \frac{7.8685}{\sqrt{2}} = 5.563 \qquad (16)$$

We see that this resolution (σ_{LE50} = 5.563 = 278ps) is even larger than that of the previous data set. This makes sense, keeping in mind that time walk effects are of greater magnitude at higher discriminator thresholds.

In order to assess the effectiveness if the time walk corrections made in the previous sections, we now measure the resolution of the counter using the corrected data. The following two histograms show the same meantime distribution for leading edge discriminators with thresholds set at 50mV. The first has been corrected with a time walk correction function of the first functional form (5) and the second has been corrected with one of the second functional form (6).

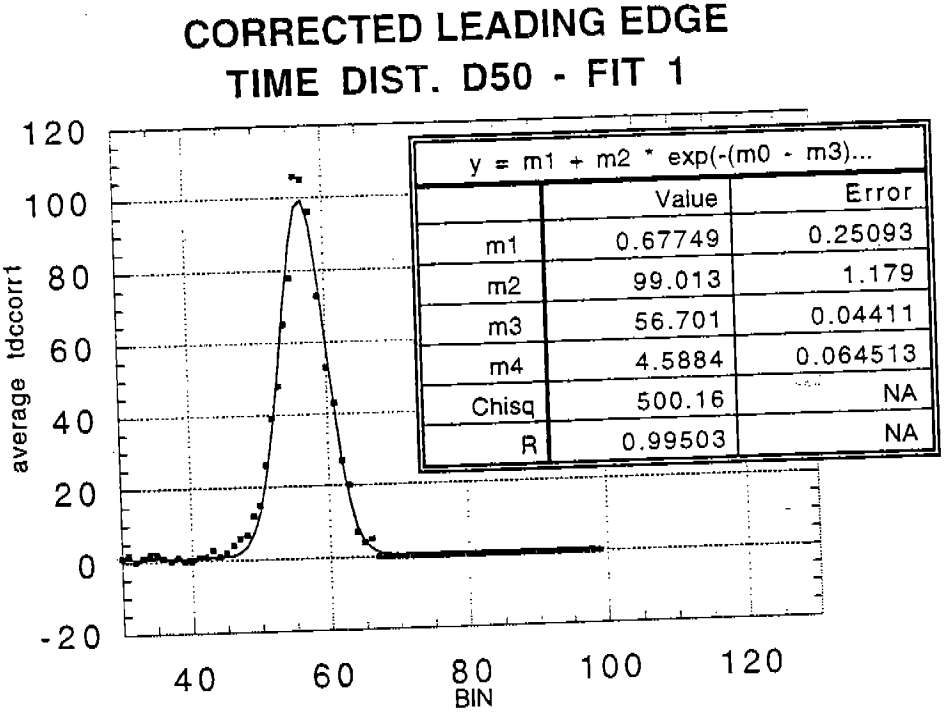

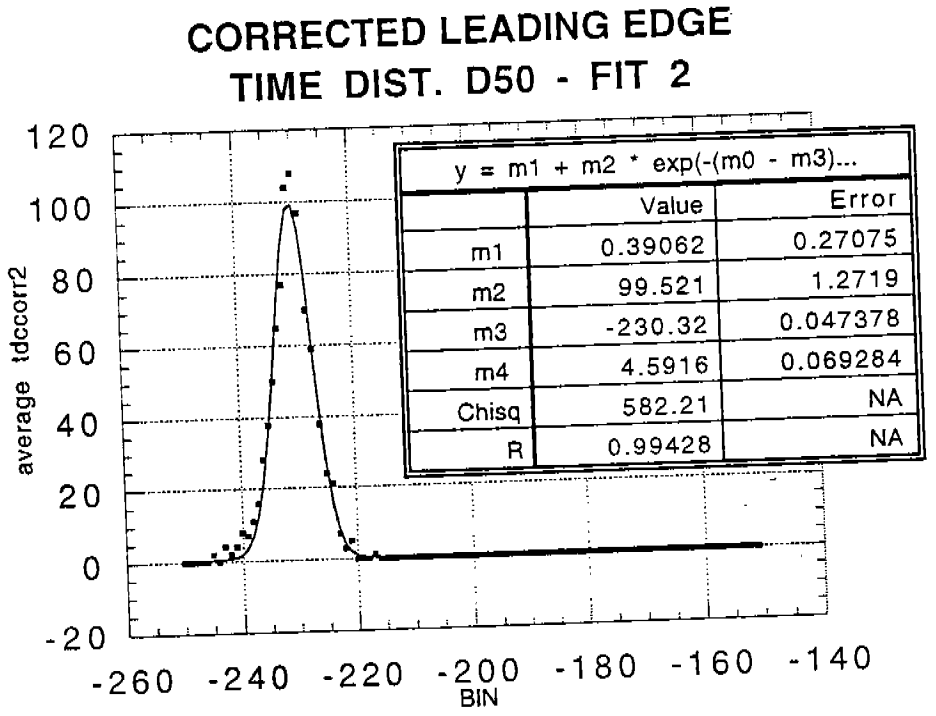

We again determine the resolutions ($\sigma_{CORR1D50}$ and $\sigma_{CORR2D50}$) of these two distributions. For the first:

$$\sigma_{CORR1D50} = \frac{4.5884}{\sqrt{2}} = 3.244 = 162ps \quad (17)$$

and for the second:

$$\sigma_{CORR2D50} = \frac{4.5916}{\sqrt{2}} = 3.247 = 162ps \quad (18)$$

From these we see that the time walk correction functions are indeed performing the task for which they were intended. The time resolution of the counter with leading edge discriminators has been improved to 162 ps with both functional forms. The corrected resolution is even smaller than the resolution of the reference data taken with constant fraction discriminators.

We perform the same measurement of resolution for the corrected data taken with thresholds at 100 mV.

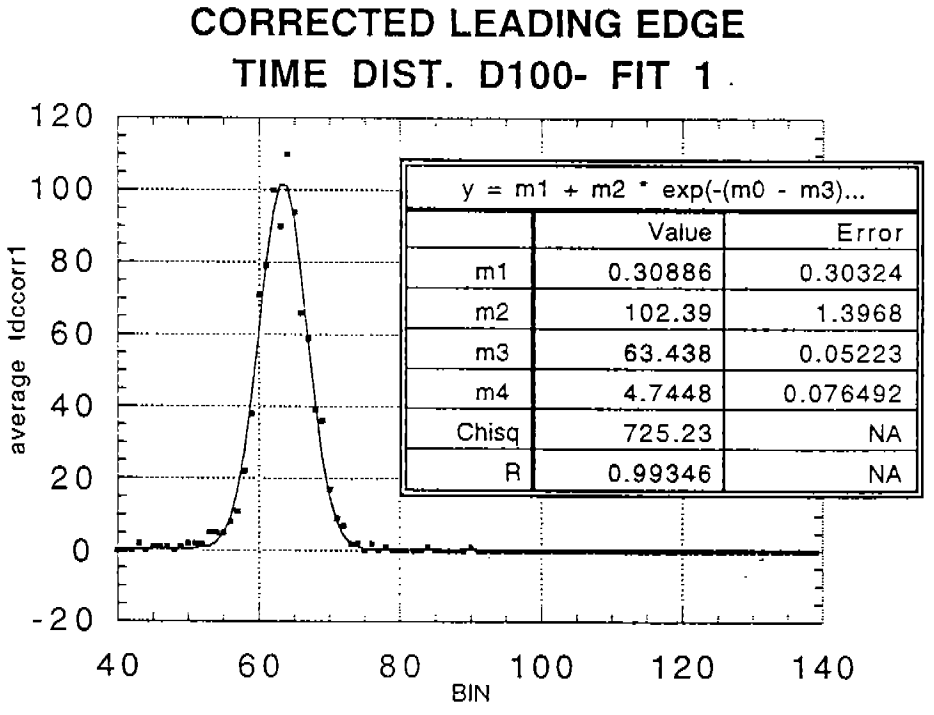

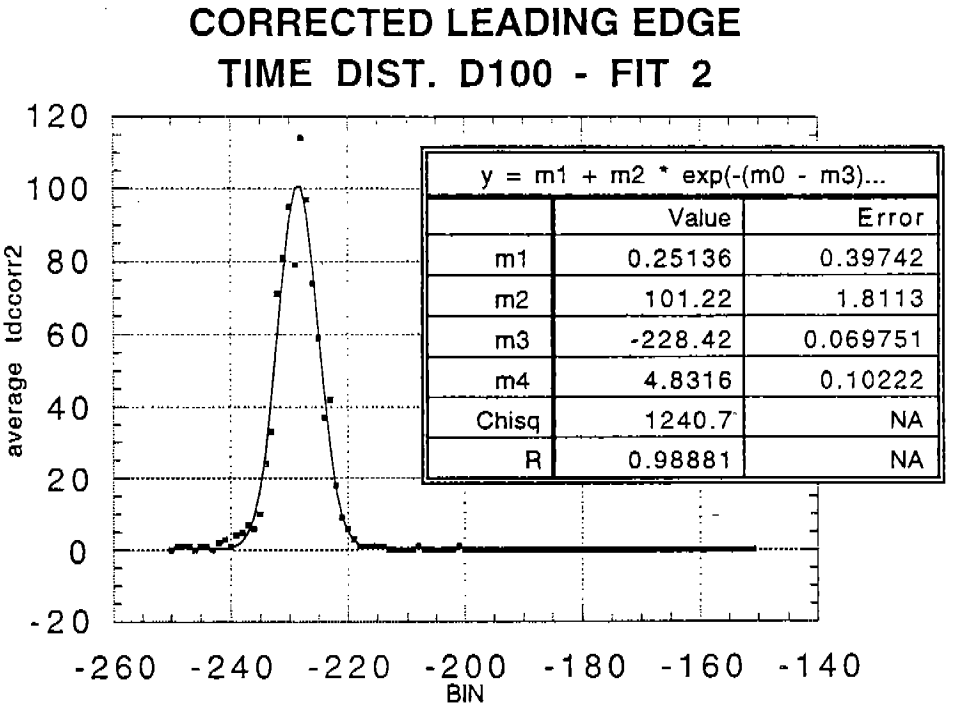

We once again determine the resolutions ($\sigma_{CORR1D100}$ and $\sigma_{CORR2D100}$) of these two distributions. For the first:

$$\sigma_{CORR1D100} = \frac{4.7448}{\sqrt{2}} = 3.355 = 167ps \tag{19}$$

and for the second:

$$\sigma_{CORR2D100} = \frac{4.8316}{\sqrt{2}} = 3.416 = 171ps \tag{20}$$

We see here that the correction functions are again performing admirably. The resolutions are a bit larger, which is to be expected due to the larger effects of time walk at larger thresholds. It is interesting to note that the more complicated functional form (fit #2) did not correct the data as well as the first functional form (fit#1). One will also notice in the corrected data with 50 mV thresholds that the resolutions are the same for both fit functions. This suggests that the simpler fit function (fit #1) corrects the data just as well and even better than the second more complicated form. The use

of the simpler function will be beneficial in reducing the computation time necessary to perform the time walk correction in software.

These results are indeed encouraging. The time walk corrections performed above improved the resolution of the counter by as much as 40%. Through these corrections it is possible to attain the timing resolution goal of 150-175ps.

3.7 ESTIMATION OF LIGHT REACHING SCINTILLATORS:

Now that we have demonstrated that it is indeed feasible to correct for time walk using this type of pulsed laser system, we can now move on to the second goal of this experiment. We will now estimate the amount of light being deposited to each scintillator if we were to repeat the experiment performed by Pavey and Perez with the new laser and new optical setup. This will involve determining a value for the total amount of light which would enter the fiber if no filters were used and subsequently dividing that value accordingly for the two levels of splitting in the Pavey and Perez experiment. From this calculation one can estimate if the new laser and optical setup will improve the system's ability to perform the calibration.

In order to make estimates of the energy equivalent of light deposited into the scintillators, we must first have some energy reference to work from. Since the overall goal of the system is to deposit an amount of light in each scintillator which will produce a pulse larger than that of a minimum ionizing particle, we will use as a reference data from our cosmic ray spectra. Cosmic rays muons, being fast (near $\beta=1$) charged particles, can be used as a minimum-ionizing energy reference. For scintillator, the amount of energy deposited by a minimum ionizing particle is about 2 MeV per gm per cm^2. The scintillator in this experiment is 5 centimeters thick and has a density of 1.032 gm/cm^3. Thus for this scintillator the energy deposited by a minimum ionizing particle is

$$E_{min} = 1.95\text{MeV}\left(\frac{\text{cm}^2}{\text{g}}\right)\left(\frac{(5\text{cm})(1.032\text{g})}{\text{cm}^3}\right) \approx 10\text{MeV} \qquad (19)$$

We can equate this minimum ionizing energy of 10 MeV with an ADC channel number by looking at an ADC spectrum from cosmic ray data. The following is such a spectrum from tube SA.

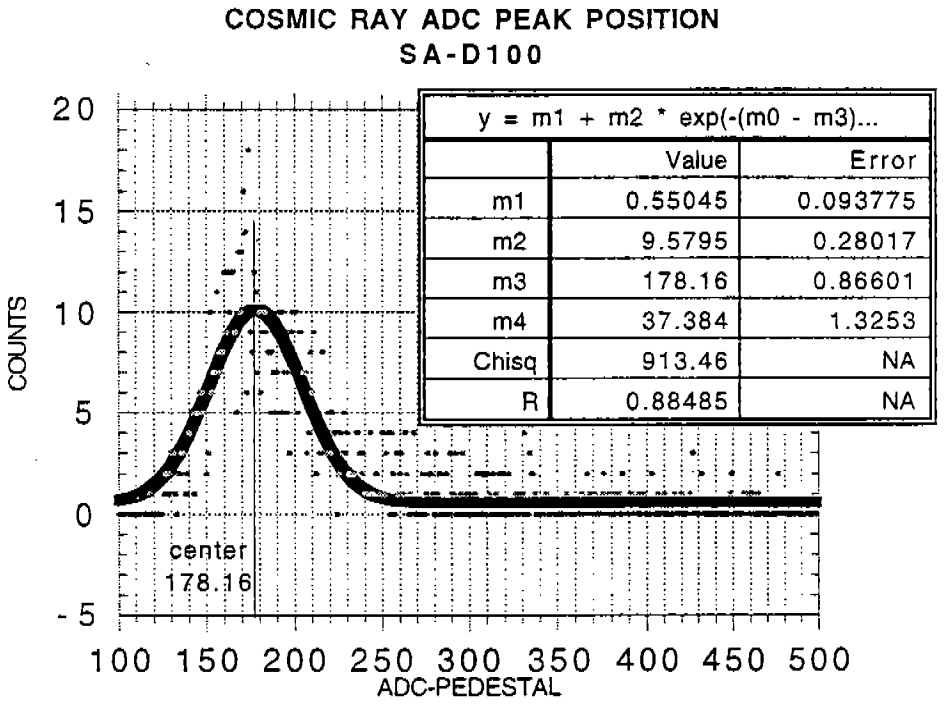

Plotted are the counts per channel for ADC values minus the pedestal. In order to determine the approximate position of the minimum ionizing energy peak, a Gaussian has been fit to the data. From the fit we see that the center of the peak is at bin 178. We equate this position with our minimum ionizing energy of 10 MeV. Assuming again that the ADC behaves linearly, we can now deduce a function relating bin number to energy. This relation is

$$\text{ENERGY} = \frac{(10\text{MeV})\text{BIN\#}}{178} \qquad (20)$$

Using this relation we can now determine the energy equivalent of the light being deposited into the scintillator for each of the laser filter settings. The following is an ADC spectrum from laser data taken by tube SA with filter #2 in the beam.

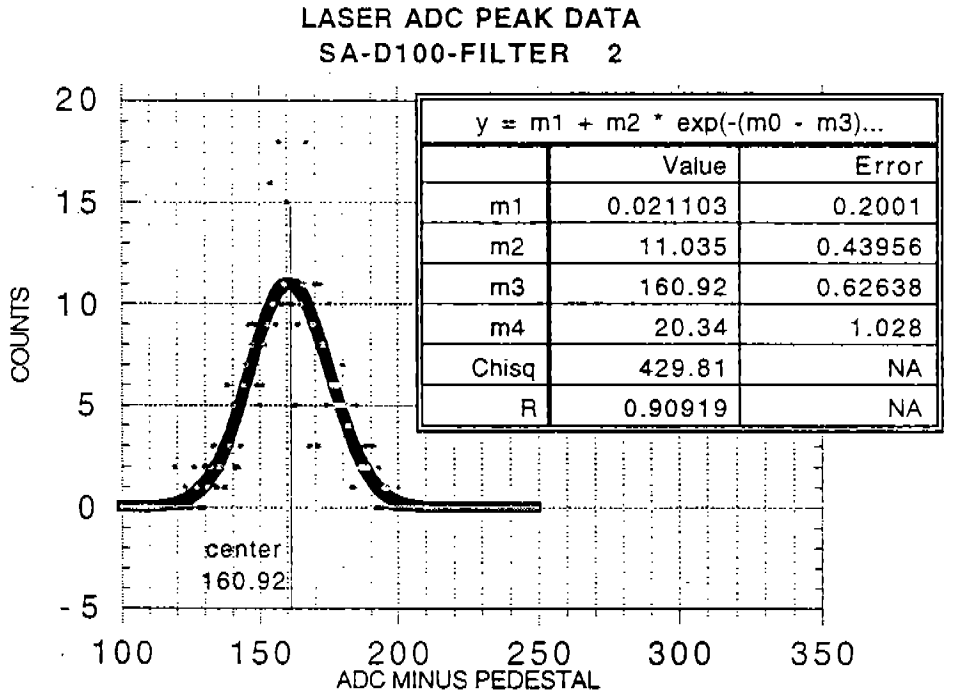

As with the cosmic ray data, a Gaussian fit has been applied and the center, channel #161) has been deduced. From relation (19) we can determine the energy equivalent of the light being deposited into the scintillator when filter #2 is in the beam.

$$E_{F2} = \frac{(10\text{MeV})161}{178} = 9.04\text{MeV} \qquad (21)$$

We perform the same fit and deduction of energy equivalent for spectra from data taken with filters 3, 4 and 5. Plots of all four of these fits with their respective centers and energy equivalents are compiled in **APPENDIX C**.

From these centers and energy equivalents we can construct the following plot which illustrates on the same scale the positions of the filter peaks and cosmic ray peak.

We then split this total energy as if we were dividing the beam with the same splitter setup as in the Pavey and Perez paper. There were two fiber splits in their research, the first being 1 to 20 and the second being 1 to 30. Each split consisted of a bundle of 100-micron fibers butted up against a large 800-micron fiber. The following is an example cross section of such a splitter where 30-100 micron fibers couple to an 800 micron fiber.

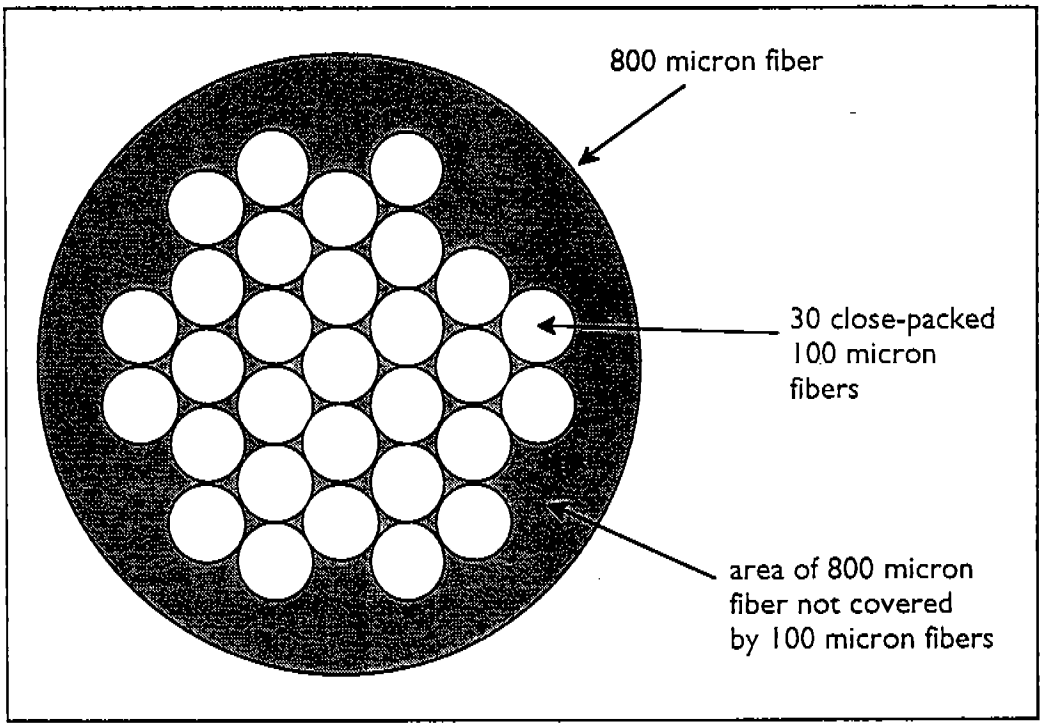

FIGURE 10: CROSS SECTION OF 1-30 FIBER SPLIT

As we can see in the diagram, which is drawn to scale, the total area of the 30-100 micron fibers is less than that of the 800-micron fiber. If light is traveling from the 800-micron fiber into the 100 micron fibers, some light will be lost in the area which the 100-micron fibers do not cover (this area is shaded gray in the diagram). The fraction of light which enters all of the 100-micron fibers from the 800-micron fiber is equal to the ratio of the total cross-sectional area of the 100-micron fibers to the cross-sectional area of the 800-micron fiber. For this bundle the ratio, which we will call R_{30}, is

$$R_{30} = \frac{30\pi(50\mu m)^2}{\pi(400\mu m)^2} = 0.47 \tag{24}$$

We calculate the same ratio R_{20} for the 1 to 20 split and obtain

$$R_{20} = \frac{20\pi(50\mu m)^2}{\pi(400\mu m)^2} = 0.31 \tag{25}$$

These ratios are calculated assuming the distribution of light across the cross section of the larger fiber is uniform at the junction with the smaller fibers. The amount of energy deposited to each scintillator E_{DEP} after these splits can then be calculated as

$$E_{DEP} = E_{TOT}R_{20}R_{30}\left(\tfrac{1}{20}\right)\left(\tfrac{1}{30}\right) = 3.21\times10^5 MeV(0.31)(0.47)(1/60) = 779MeV \tag{26}$$

Based upon this estimation there will certainly be adequate light reaching the scintillators. This value of 779 MeV does not, however, take into account the attenuation due to fiber length. In the Pavey and Perez research, the laser light traveled through no more than 5 meters of fiber before reaching the scintillator. This is a loss of 1.5 dB (29% of the light was lost due to fiber attenuation). Thus, we would expect a light pulse equal to 0.71x779 MeV, or 551 MeV to reach each scintillator. This is over 55 times the minimum ionizing energy of 10MeVwhich is a very encouraging result.

4. CONCLUSIONS AND FURTHER RESEARCH

The experimentation performed in this research accomplished quite well the goals for which it was designed. First, it was determined that it is indeed feasible to correct for time walk in the timing measurements made by the time-of-flight scintillation counters using a pulsed nitrogen laser. These corrections make it possible to achieve a timing resolution of 150-175 picoseconds without the trouble of maintaining constant fraction discriminators. Second, it was determined that with the use of a new more powerful laser and a more efficient optical setup to direct the laser into optical fibers, the amount of light deposited to each scintillator in the proposed system would be adequate for calibration. In these regards this research was a success.

The further understanding of this calibration system will require more extensive research developing upon that performed here. Now that it has been shown that time walk correction is indeed feasible, it must be better understood for more general cases and for larger data sets. This research is currently being performed (Summer 1995) at CEBAF by using the laser calibration system in conjunction with the cosmic ray test of one section of the CLAS calorimeter.

5. ACKNOWLEDGMENTS

I would like to thank Professor Dayle Hancock, Professor John Kane, an Professor Morton Eckhause at the College of William and Mary for their help in completing this thesis. I would also like to thank Elton Smith at CEBAF for all of the time and effort he contributed to this thesis. I would also like to thank Kirk Jacobs in the William and Mary physics machine shop for doing good work on short notice. Thanks also to those who put together the CLAS internet homepage which provided the nice illustrations in figures 1 and 2.

6. REFERENCES

"Application Note AN-5: Time-of-flight Measurements and Leading Edge Timing Compensation." LeCroy Corporation. New York. 1983.

Pavey, T.G. Senior Honors Thesis. College of William and Mary. Williamsburg, VA. 1993. (unpublished)

Perez, R. Senior Honors Thesis. College of William and Mary. Williamsburg, VA. 1993. (unpublished)

S. Banjeree et al. "Design and Performance of a Time-of-Flight System for Particle Identification at the Fermilab Collider." **Nuclear Instruments and Methods in Physics Research**. A269. 1988. p129.

APPENDIX A: TDC VS ADC PLOTS

The following are all plots comparing TDC and ADC values in the laser data sets taken in this experiment. The plots show the relation between TDC and ADC values for compiled events from data sets taken for filters 2 through 5. For each compiled data set there are two plots, each with a fit to one of the two functional forms as shown in equations (5) and (6). The results of these fits are given for each plot.

The following plots are for tube SA with discriminator levels set at 100 mV.

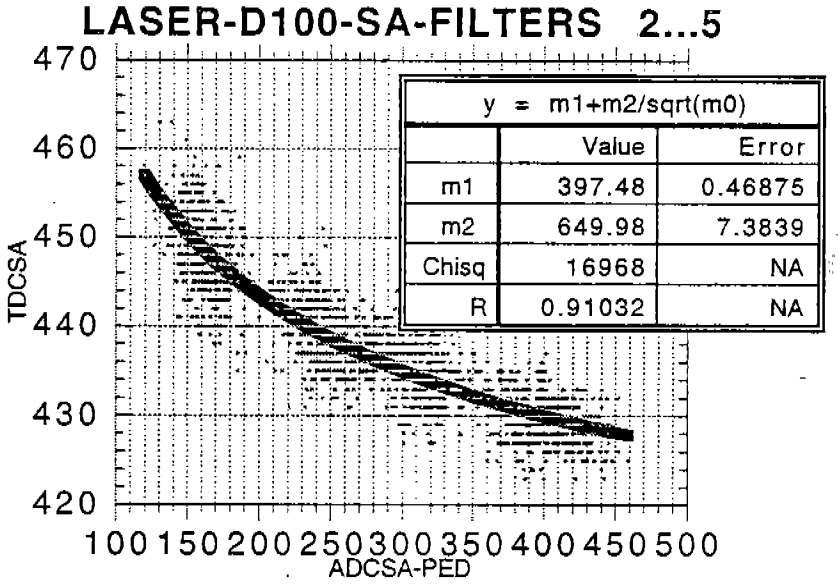

$$TDC = 397.48 + \frac{649.98}{\sqrt{ADC}}$$

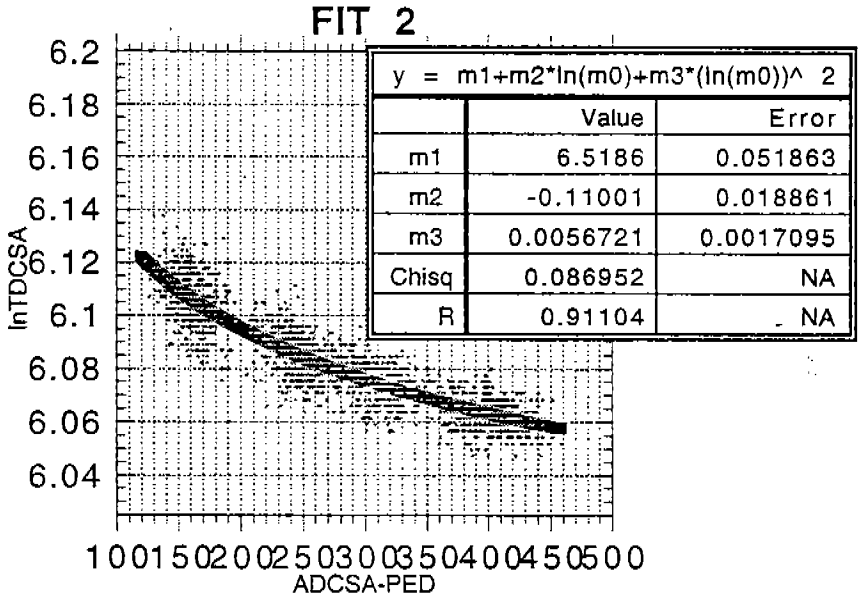

$$\ln(TDC) = 6.51860 - 0.11001(\ln(ADC)) + 0.0056721(\ln(ADC))^2$$

The following plots are for tube SB with discriminator levels set at 100 mV.

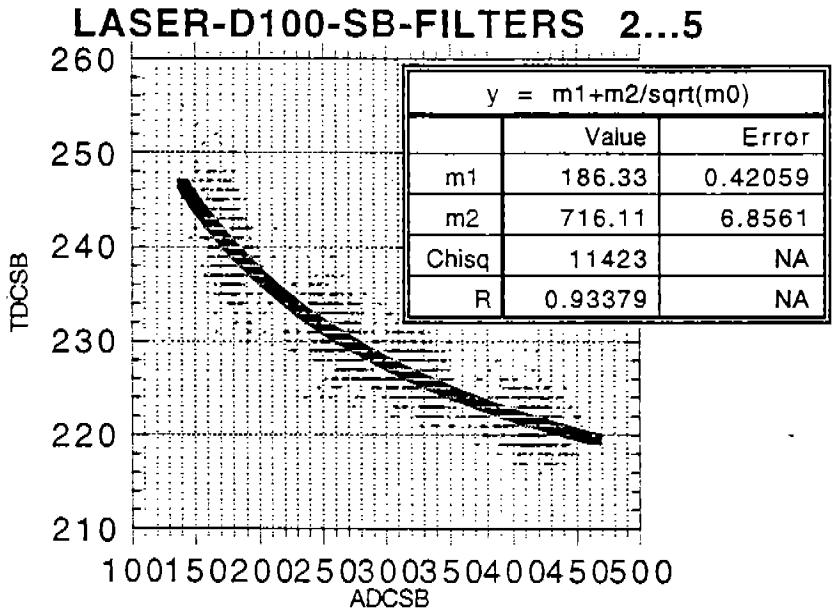

$$TDC = 186.33 + \frac{716.11}{\sqrt{ADC}}$$

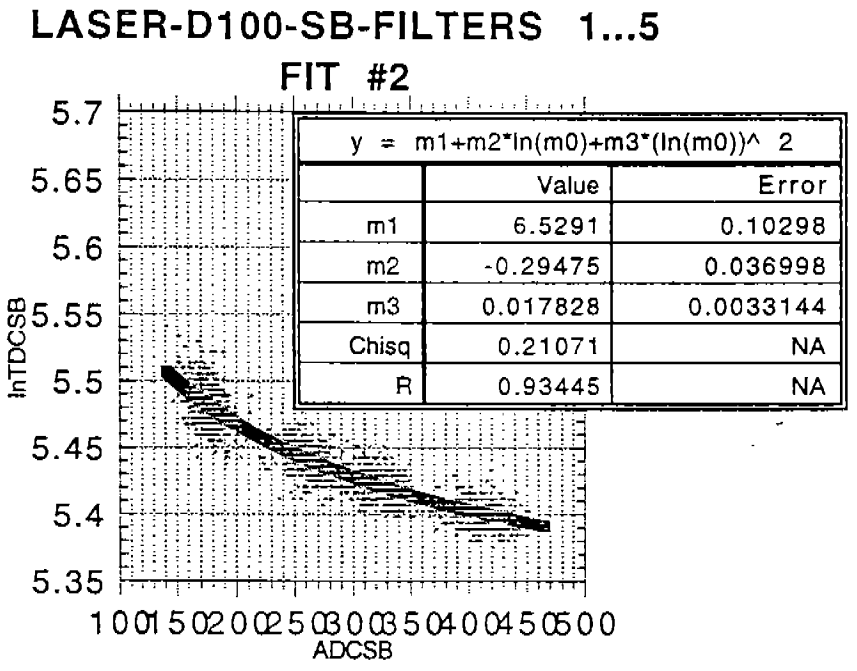

$$\ln(TDC) = 6.5291 - 0.29475(\ln(ADC)) + 0.0178281(\ln(ADC))^2$$

The following plots are for tube SA with discriminator levels set at 50 mV.

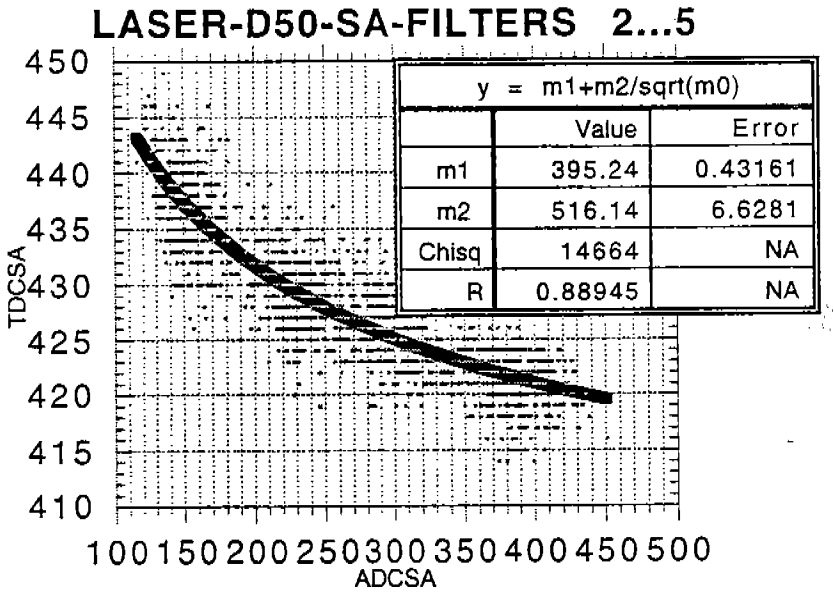

$$TDC = 395.24 + \frac{516.14}{\sqrt{ADC}}$$

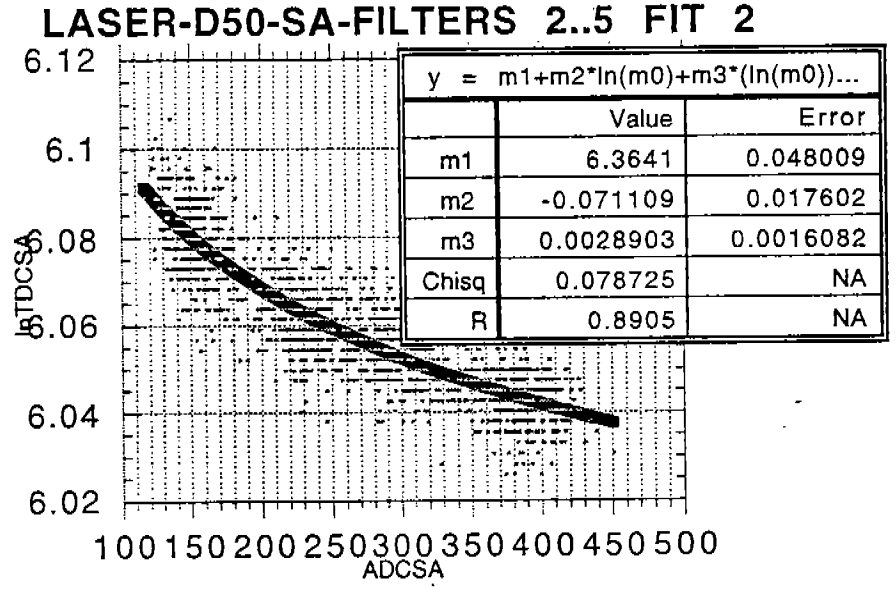

$$\ln(TDC) = 6.3641 - 0.071109(\ln(ADC)) + 0.0028903(\ln(ADC))^2$$

The following plots are for tube SB with discriminator levels set at 50 mV.

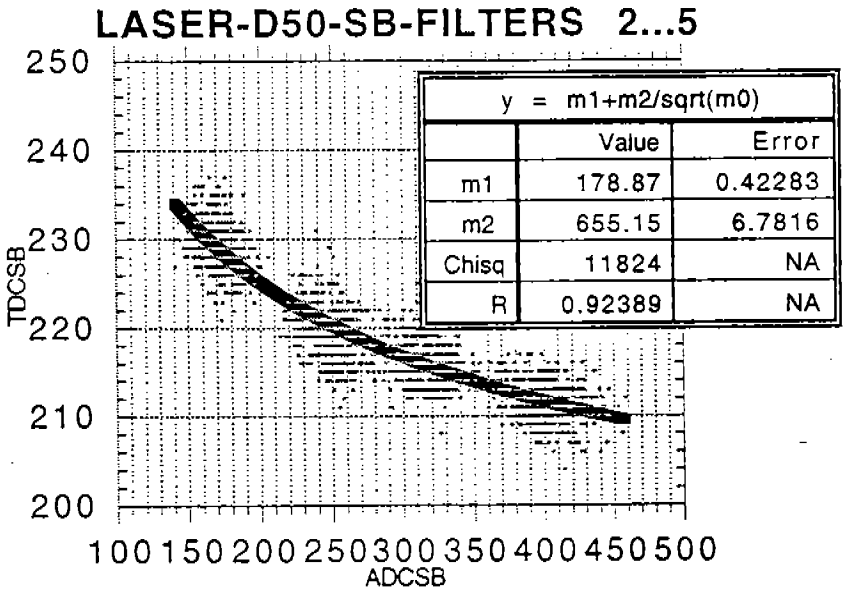

$$TDC = 178.87 + \frac{655.15}{\sqrt{ADC}}$$

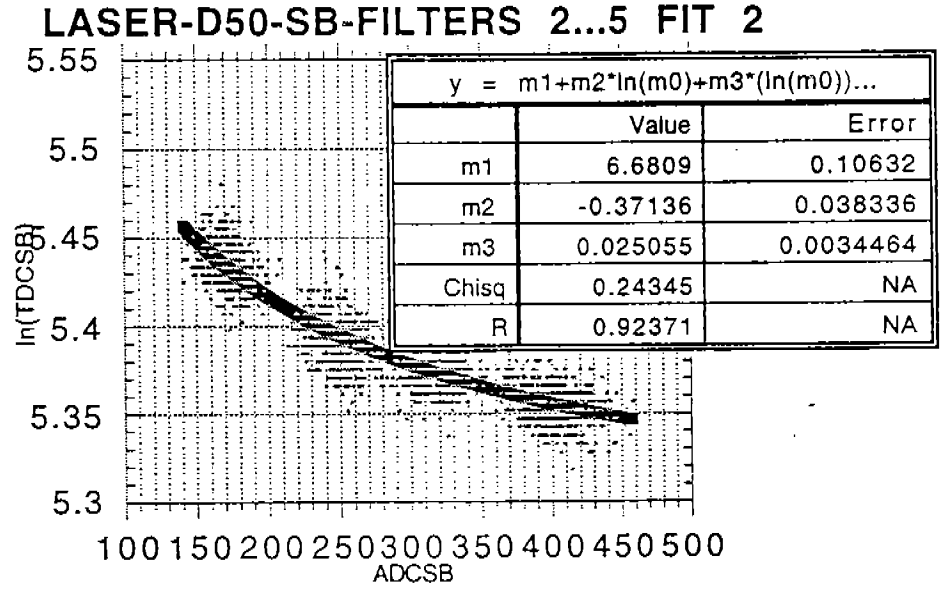

$$\ln(TDC) = 6.6809 - 0.037136(\ln(ADC)) + 0.025055(\ln(ADC))^2$$

APPENDIX B: COSMIC RAY DATA SETS WITH TIME WALK CORRECTIONS APPLIED

The following sets of graphs show the relation between pulse height and timing for the cosmic ray data sets taken for both tubes. Sets are shown for both discriminator levels and types of discriminator (constant fraction and leading edge). For each tube, the raw leading edge and constant fraction data are plotted, along with the corrected leading edge data produced by the two corresponding experimentally determined time walk correction functions. One will notice that the correction functions applied to the leading edge data removed the time dependence, rendering them similar to the constant fraction data.

The following graphs are for tube SA with a discriminator threshold of 100mV.

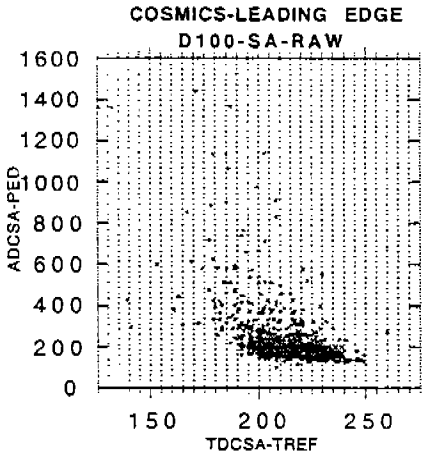

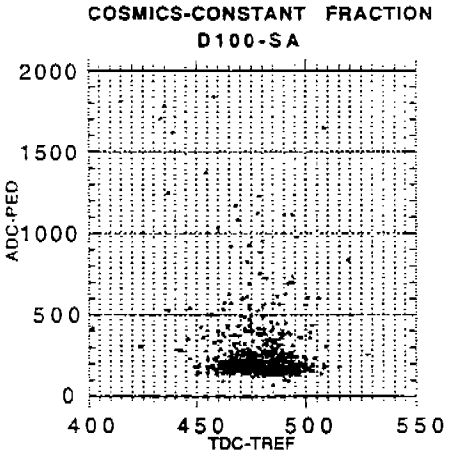

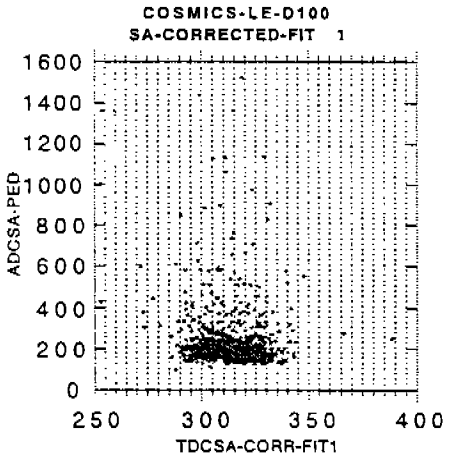

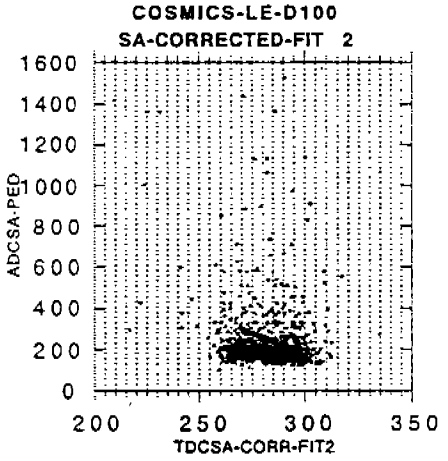

The following graphs are for tube SB with a discriminator threshold of 100mV.

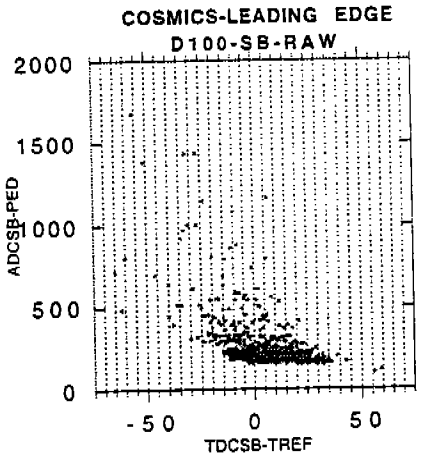

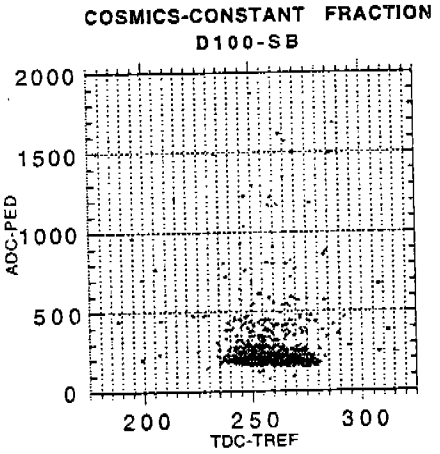

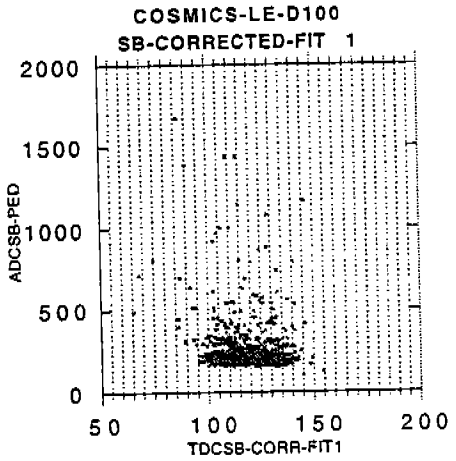

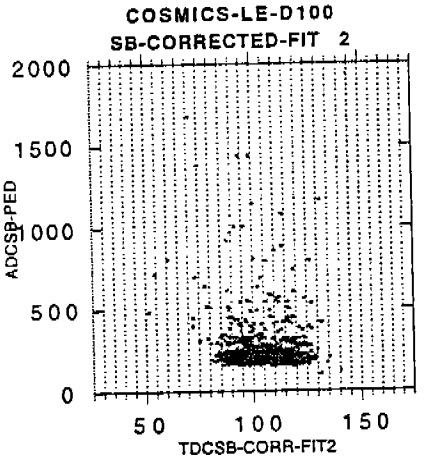

The following graphs are for tube SA with a discriminator threshold of 50mV.

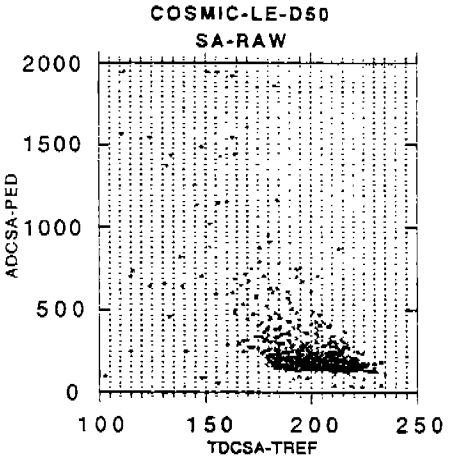

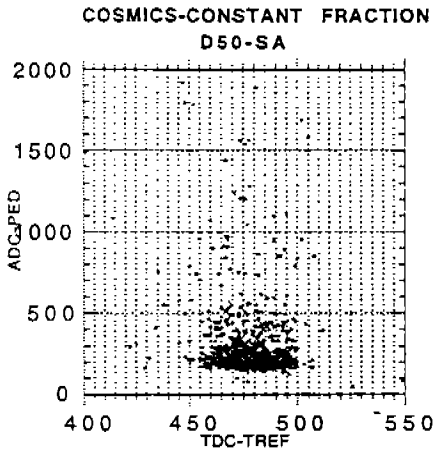

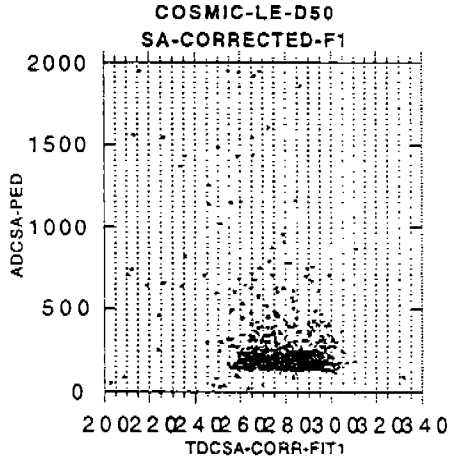

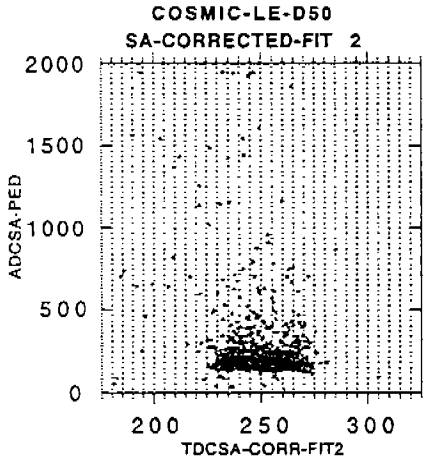

The following graphs are for tube SB with a discriminator threshold of 50 mV.

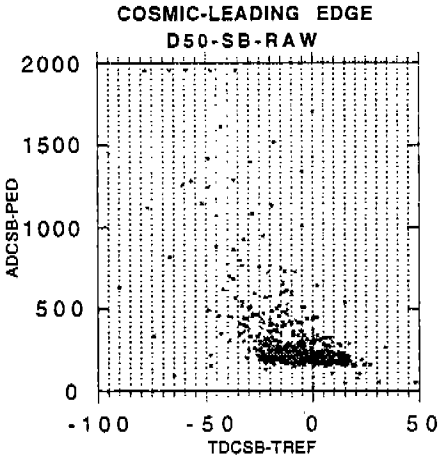

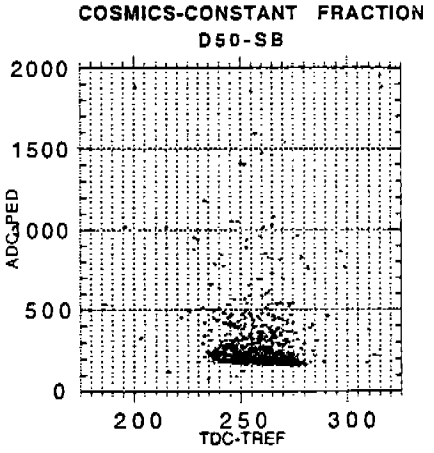

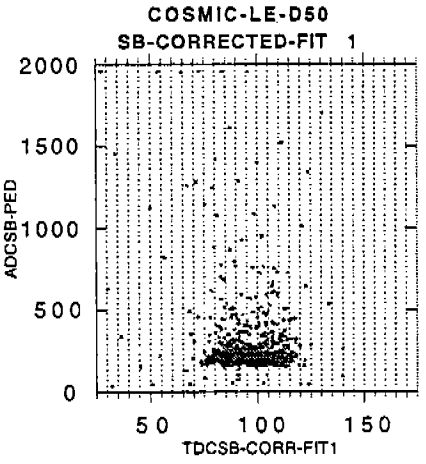

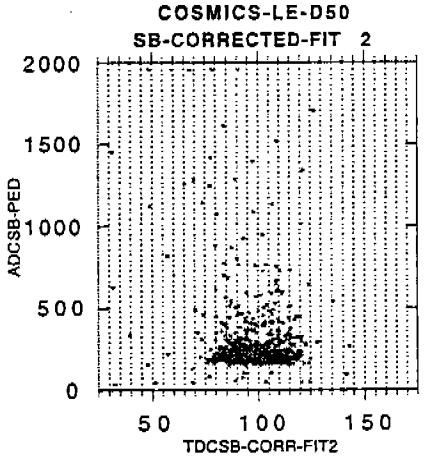

APPENDIX C: LASER ADC SPECTRA WITH CENTERS AND ENERGY EQUIVALENTS

The following plots show ADC spectra for laser data taken with tube SA for filters 2 through 5. Gaussian fits have been applied in each case from which peak centers have been determined. Energy equivalents of these center positions are then determined using relation (19).

LASER ADC PEAK DATA
SA-D100-FILTER 2

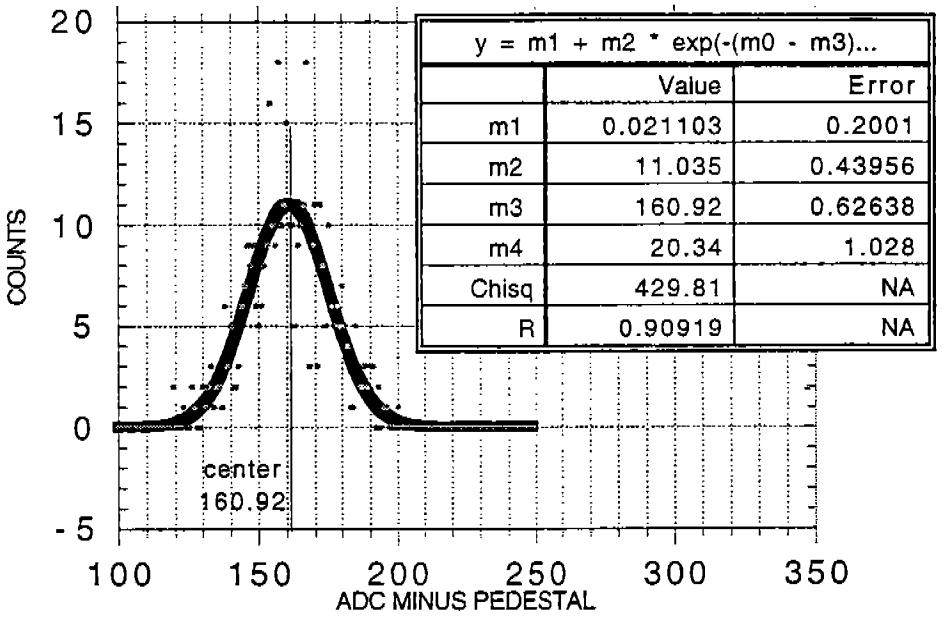

$$E_{F2} = \frac{(10MeV)161}{178} = 9.04MeV$$

LASER ADC PEAK DATA
SA-D100-FILTER 3

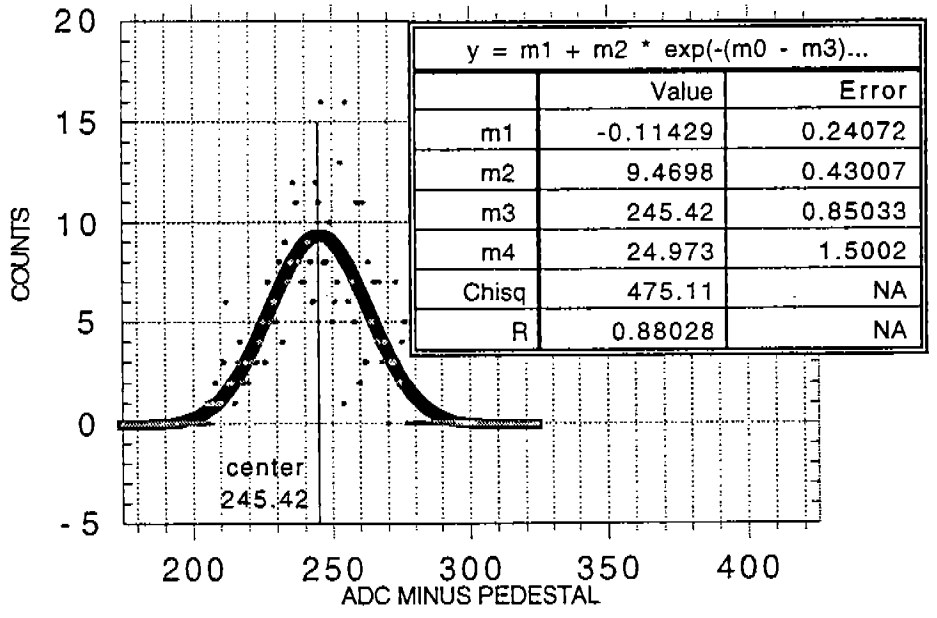

$$E_{F3} = \frac{(10MeV)245}{178} = 13.8MeV$$

LASER ADC PEAK DATA
SA-D100-FILTER 4

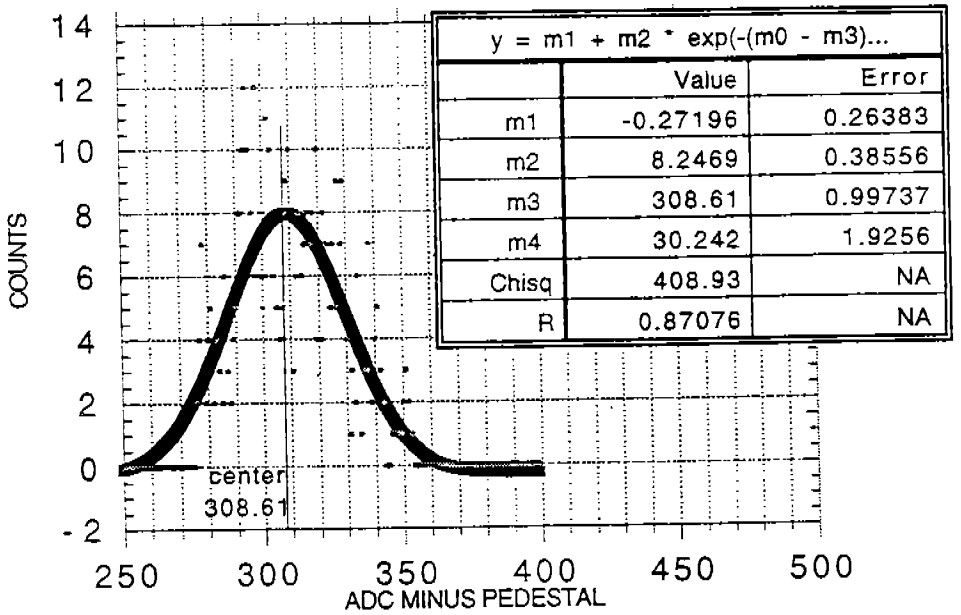

$$E_{F3}=\frac{(10MeV)309}{178}=17.4MeV$$

LASER ADC PEAK DATA
SA-D100-FILTER 5

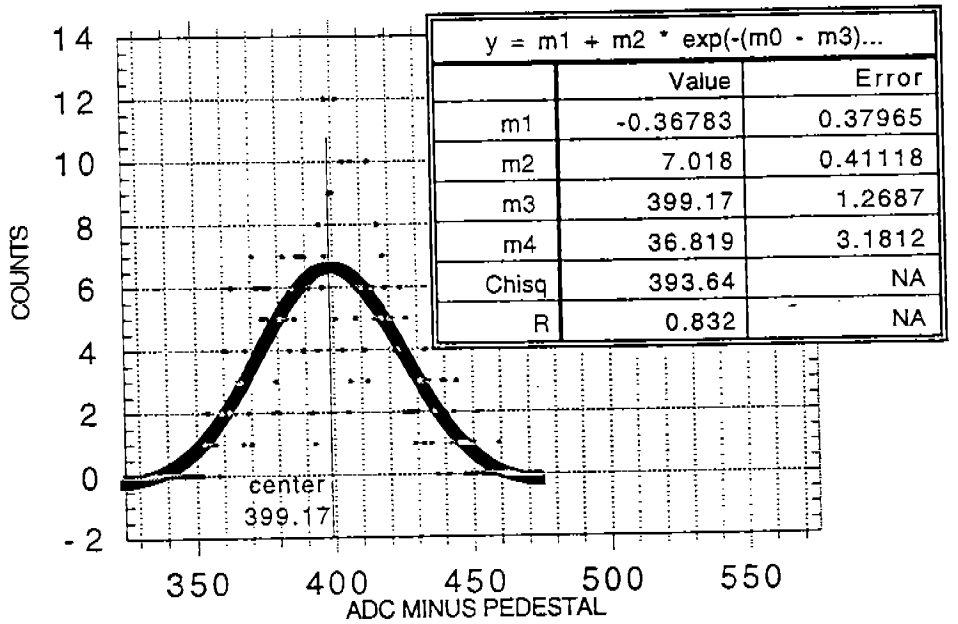

$$E_{F3}=\frac{(10MeV)399}{178}=22.9MeV$$